

Project Number: AS5 AAEJ



Application of Phase Change Materials in Airport Runways

A Major Qualifying Project Report
Submitted to the Faculty
of the

WORCESTER POLYTECHNIC INSTITUTE

in partial fulfillment of the requirements for the

Degree of Bachelor of Science

By

Paul R. Bender, Civil Engineering

Sarah A. Cote, Civil Engineering

Rachel A. Lewis, Mechanical Engineering

Bryan J. Manning, Mechanical Engineering

Date: March 25, 2014

Approved:

Professor Aaron R. Sakulich, Project Advisor

Professor Rajib B. Mallick, Project Co-Advisor

Acknowledgements

We would like to express our appreciation to Professors Aaron R. Sakulich and Rajib B. Mallick for their valuable and constructive suggestions during the entire project. Their guidance enabled us to navigate the multiple obstacles encountered during this project.

We would like to also thank Russell Lang, Gregory Freeman, Naser Sharifi, and Ryan Worsman for their help during the project. Their experience and guidance enabled us to fully utilize the resources of the Civil Engineering Department and lab facilities.

In addition, we would like to thank Sarah Dennechuk (Massport), John Kirkendall (Jacobs Engineering), Jonathan Neeser (Worcester Airport), and Barry Hammer (FAA Airports Division) for their interviews about airport pavements. With their expertise, we were able to better focus our research towards solving problems directly affecting airports.

We would also like to thank Northeast Solite Corporation for the donated lightweight aggregate that was used to construct our samples.

Authorship

Paul R. Bender was responsible for formatting the report and contributed to the background, methodology, and results sections. His topics included hot mix asphalt, phase change materials, and sample mixing, production, and volumetric testing. He also drafted the mix designs, organized lab batching and production operations, and contributed to the volumetric and thermal testing of samples.

Sarah A. Cote was responsible for editing and formatting the project poster, and writing the discussion about the capstone design requirements. She also contributed to writing the background, methodology, and conclusion, drafting mix designs, and constructing and testing the samples.

Rachel A. Lewis was responsible for writing the methodology and results of Phase 1, the evaporation and absorption test sections. She also contributed to the formatting of the paper, as well as the sample production and testing procedures.

Bryan J. Manning was responsible for writing the methodology and analyzing the results from the Phase 2 and Phase 3 GLC data. He also contributed to construction and physical testing of the samples, and investigated improvements to the GLC. Additionally, he contributed to proofreading and editing the entire report.

Abstract

The purpose of this project was to explore the feasibility of incorporating phase change material (PCM) into hot mix asphalt (HMA) as a method for reducing damage caused by thermal stresses in airport pavements. The incorporation of PCM was expected to improve safety by reducing debris from deteriorating pavement, improve the state of the runway by lessening damages, and decrease the amount of time, money and resources needed to maintain runways. PCMs release or absorb heat which makes the material ideal for regulating temperature. The release or absorption of heat occurs during the phase change and can be used to reduce thermal stresses and damage in pavements. For this project, PCM-6 was utilized because the phase change temperature occurred at 6 °C.

First, combustion, absorption, and evaporation tests were conducted to determine how PCM-6 would behave under the high temperatures associated with asphalt mixing. Test cubes were constructed with several concentrations of PCM-6 to determine the feasibility of using lightweight aggregate (LWA) as an absorption medium for incorporating PCM-6 into HMA. Next, the thermal properties of the samples were evaluated using a Guarded Longitudinal Calorimeter (GLC) to generate a fluctuating heat flow and measure temperatures of the sample. After selecting a final mix design, another batch of samples was produced and subjected to theoretical maximum density tests, bulk specific gravity tests, and an improved GLC test procedure. Phase 1 and Phase 2 data indicated it was possible to incorporate concentrations up to 2.5% PCM-6 by mass into HMA, but larger amounts of PCM-6 caused a loss of all structural integrity. Thermal tests determined the incorporation of PCM slowed the rate of cooling and reduced the extreme temperatures reached, but did not completely prevent freezing. Further research should be conducted to investigate PCM incorporation methods, develop improvements to the mix design, and experiment with different types of PCMs and thermal cycling.

Capstone Design Statement

The design problem addressed in this project was to evaluate the effectiveness of utilizing phase change materials (PCMs) as a method to reduce thermal stress in hot mix asphalt (HMA) pavements. As a novel field of engineering design research, this project involved several iterative processes and multiple steps of feasibility tests. First, it was critical to assess if a PCM could withstand the high temperatures associated with mixing HMA without combusting or completely evaporating. It was also necessary to test different gradations of lightweight aggregate (LWA) for absorption to determine whether PCM would be absorbed by the LWA or adhered to the surface, as well as to determine the capacity of the LWA to absorb PCM. This data was used to select the best blend and amount of LWA based on the amount of PCM required in each sample. Once a workable heating time and LWA blend were selected, an iterative design process was completed to determine a feasible concentration of PCM that could be incorporated without compromising the structural integrity of the samples. Using these initial results, the mix design was recalculated in accordance with the Superpave specification, which involved selecting a proper aggregate gradation and binder content for optimal volumetric properties. In this way, the design problem was approached using an iterative process in order to eliminate variables and accurately study the feasibility of incorporating PCM into HMA.

The challenges of incorporating PCM into HMA involve economic, environmental, sustainability, manufacturability, and health and safety constraints. The economic problems of incorporating PCM into HMA include the fact that the savings from reducing the frequency and scale of runway maintenance must exceed the cost of incorporating the PCM. Furthermore, the frequency at which a runway needs to be repaved or sealed has a direct effect on the environment and air quality because harmful chemicals are released during these maintenance processes. Therefore, it is more environmentally friendly to have pavement that withstands temperature changes and needs to be replaced less routinely. It is also more sustainable to build pavements that do not need to be replaced as often because fewer materials are wasted long-term. Manufacturability was also a constraint in the design process because there were many issues encountered with the incorporation method for the PCM. The PCM should ideally be incorporated in a way or at a ratio which will not compromise the strength of the pavement, and which will not adversely affect the hot mixing process. In terms of health and safety, it is imperative to keep runways free of debris of any size. Failing pavement that chips off of a

runway poses a danger to aircraft during both landing and takeoff; therefore, developing a pavement that is less susceptible to thermal damage could keep runways safer. In this way, the design experience also involved taking realistic constraints into consideration during the problem solving process.

Executive Summary

Scope of Work

Having well-maintained and safe runways is pivotal in ensuring the ability of the aviation industry to function safely and economically. The purpose of this project was to explore the feasibility of incorporating phase change materials (PCMs) into hot mix asphalt (HMA) as a method for reducing damage from thermal stresses in airport pavements. The incorporation of PCM was expected to improve safety by reducing debris from deteriorating pavement, therefore decreasing the amount of time, money and resources necessary to maintain runway pavements.

Phase Change Materials and Hot Mix Asphalt

PCMs are temperature regulating materials that have the ability to release or absorb heat. The release or absorption of heat occurs during the phase change, which makes the proper selection of a PCM largely dependent on the temperature at which the phase change occurs. In this project, PCM-6 (a blend of paraffin waxes) was used as it underwent a phase change at 6 °C. The phase change temperature was above the freezing temperature of water which meant it could potentially be used to prevent thermal stresses and damage in pavements. At room temperature, the PCM is liquid, but as the temperature lowers to 6 °C, the material undergoes an exothermic phase change and solidifies. Conversely, when the system warms, the phase change material becomes endothermic and liquefies. The amount of heat that is either released or absorbed during these transition periods depends on the latent heat of fusion of the PCM. Materials with a high latent heat can delay a temperature change in their environment for a longer period of time.

To assess how PCM could potentially improve the quality of runways, it was important to understand the types of failure mechanisms of HMA. HMA can fail in four primary modes: cracking, disintegration, distortion, and loss of friction. Causes of cracking include fatigue due to load, thermal fluctuations, or a combination of both; reflection cracking due to underlying layers; and freeze-thaw action due to infiltrated water in the pavement. Disintegration often results from freeze-thaw action at potholes or patches, or from jet blast erosion on the pavement surface. Distortion results from deformation in any of the layers of the pavement structure or the subgrade. Loss of friction can occur if binder bleeds to the pavement surface during hot weather or if materials such as rubber accumulate on the surface of the pavement and cause it to be too smooth for traffic. The primary modes of failure investigated in this project were low-

temperature related distresses including low-temperature cracking, thermal fatigue cracking, and cracking due to freeze-thaw cycling in a water-infiltrated pavement.

Low-temperature cracking occurs when a pavement experiences extreme cold temperatures that are outside of the operating range of the binder. This exposure forms microcracks, which reduce the tensile strength of the HMA and initiate crack formation. If temperatures remain such that low-temperature cracking does not occur because the tensile strength is not exceeded, the HMA will not fail immediately. However, strains may build up after repeated high- and low-stress cycles produced by temperature fluctuations and traffic loading over time. These fluctuations could lead to failure in the long-term by thermal fatigue cracking. These repeated stress cycles are often inevitable over the lifetime of a pavement. PCMs may be able to reduce a pavement's susceptibility to low-temperature and thermal fatigue cracking. As the temperature of the pavement decreases, the PCM will freeze and release heat into the matrix keeping the system warmer than the ambient temperature. If a pavement contained a PCM with a low enough melting point, the PCM could temporarily prevent the pavement from crossing or approaching the operational threshold of the binder, depending on the frequency and intensity of low temperature cycles. In this way the PCM can reduce the extremes of temperature fluctuation and make pavement temperature profiles smoother. This smoother profile may also help to deter freeze-thaw cycling in pavements that have absorbed water.

Methodology

In order to gain specific information on common types of thermal damages to airport pavements, professionals with knowledge of airport pavements were contacted. Questions were geared to each recipient's location and areas of expertise, and were developed in order to gain a range of information. The respondents included John Kirkendall (Jacobs Engineering), Jonathan Neeser (Worcester Airport), and Barry Hammer (FAA Airports Division). From the interviews, the decision was made to focus on the effects of water penetration of HMA pavements through surface cracks. By reducing crack initiation at the surface, the number of entry points for water to penetrate the pavement is reduced. Thus, to attempt to provide a solution for surface crack reduction, it was decided to pursue low-temperature PCM effects in HMA pavements.

PCM-6 had not been previously used with HMA, and the proposed method of incorporation of the PCM-6 (via absorption into a porous lightweight aggregate [LWA]) posed some initial concerns for the hot mixing process. Therefore, before attempting to incorporate

PCM-6 into HMA, uncertainties in the behavior of PCM-6 were investigated. Phase 1 testing included placing a beaker containing 20 mL of PCM-6 into an oven at 150 °C to simulate the conditions of mixing HMA in order to determine if the material would ignite. After determining that the material would not ignite, absorption and evaporation tests were conducted to determine how much PCM-6 was absorbed by the LWA and how much evaporated during the HMA mixing process. During Phase 2 testing, test cubes including control and PCM/HMA samples were produced to assess the feasibility of utilizing LWA to incorporate PCM-6 into HMA. To assess the feasibility, qualitative observations were recorded on the appearance of the sample and thermal properties were evaluated using a Guarded Longitudinal Calorimeter (GLC). In Phase 3, a final mix design was selected in an attempt to comply with the Superpave specification and the GLC testing protocol was modified. Both changes were to address issues with Phase 2 testing. A final batch of samples was produced and subjected to theoretical maximum density tests, bulk specific gravity tests, and an improved GLC test procedure.

Conclusions

The incorporation of PCM-6 into HMA using LWA was shown to be possible, but was not yet feasible for use in airports. The collected data provided evidence that the incorporation of PCM altered the thermal properties of the sample, but this integration came at the cost of the strength of the sample. Although no strength tests were conducted on the samples, many of them were easily damaged during testing and handling. Further research should be conducted to determine the effects of LWA on the mechanical properties of the HMA and to determine the interaction between the PCM and the binder. Other methods of introducing PCMs into HMA should be investigated that isolate the PCM from the binder, such as encapsulating the PCM in a pellet, while still dispersing it throughout the matrix of the structure. In addition, the volumetric property testing completed in Phase 3 indicated that PCM-6 did not have an adverse effect on volumetric properties, such as air voids, when compared to a control sample. However, this should be verified using the proper Superpave mix production procedure instead of the hand compaction methods used in this study. Testing for both the volumetric and thermal properties of individual samples may be facilitated if the GLC was altered to work with cylindrical samples.

Overall, both Phase 2 and Phase 3 testing provided insight that it was possible to incorporate PCM-6 into HMA using LWA. The data showed that PCM reduced the extreme low temperature of a sample, reduced the rate of cooling, and decreased the time for the sample to

thaw. Initially, PCM-6 was selected because it had a phase change temperature above the freezing point of water, which meant it could potentially prevent freezing and, thus, freeze-thaw cycling. In reality, after assessing the data from Phase 2 and Phase 3, it was found that the PCM was not able to prevent freeze-thaw cycling and that samples behaved differently when subjected to slower or quicker cooling/heating cycles. For future tests, different cooling/heating cycles and types of PCM should be tested to better understand how the PCM responds to different extreme temperatures and temperature cycling. For instance, one experiment might test a PCM sample with a gradual cooling rate that reaches an extreme cold temperature, while another might explore a quick cooling rate that reaches a less-extreme cold temperature. Having a better understanding of the response of the PCM will be useful in deciding which PCM is suited for given conditions. Potentially, composite samples comprised of multiple types of PCM could be designed in order to contend with different temperature conditions. Thus, there is a need for further research on this topic in order to improve the feasibility of incorporating PCM into HMA for use in airport runways.

Table of Contents

Acknowledgements.....	i
Authorship.....	ii
Abstract.....	iii
Capstone Design Statement	iv
Executive Summary	vi
Scope of Work.....	vi
Phase Change Materials and Hot Mix Asphalt	vi
Methodology	vii
Conclusions.....	viii
Table of Contents.....	x
List of Figures.....	xiii
List of Tables	xv
Glossary of Terms.....	xvi
1 Introduction	1
2 Background.....	4
2.1 Foreign Object Debris (FOD)	4
2.2 Properties of Hot Mix Asphalt (HMA)	4
2.3 Pavement Distresses.....	6
2.4 Pavement Treatments	8

2.5	Airport Pavement Maintenance.....	9
2.6	Phase Change Materials (PCMs).....	10
2.7	Rutting and Thermal Cracking in HMA	11
3	Methodology.....	15
3.1	Evaluation of Facility Problems and Definition of Project Scope	15
3.2	Experimental Methods Summary.....	16
3.3	Phase 1: Heating and Evaporation Tests	17
3.4	Phase 2: Sample Production and Thermal Testing.....	18
3.4.1	<i>Sample Production</i>	18
3.4.2	<i>Guarded Longitudinal Calorimeter</i>	19
3.4.3	<i>GLC Testing in Phase 2</i>	21
3.5	Phase 3: Improved Mix Design with Volumetric and Thermal Testing	22
3.5.1	<i>Aggregate Gradation Analysis</i>	22
3.5.2	<i>Theoretical Maximum Density Test, Sample Mix Design, and Production</i>	22
3.5.3	<i>Bulk Specific Gravity Test and Volumetric Calculations</i>	23
3.5.4	<i>GLC Testing in Phase 3</i>	23
4	Results and Discussion	25
4.1	Phase 1: Heating and Evaporation Tests	25
4.2	Phase 2: Sample Production and Thermal Testing.....	27
4.2.1	<i>Sample Production and Mix Designs</i>	27

4.2.2	<i>GLC Testing in Phase 2</i>	29
4.3	Phase 3: Improved Mix Design with Volumetric and Thermal Testing	35
4.3.1	<i>Aggregate Gradation Analysis</i>	35
4.3.2	<i>Theoretical Maximum Density Test, Sample Mix Design, and Production</i>	37
4.3.3	<i>Bulk Specific Gravity Test and Volumetric Calculations</i>	37
4.3.4	<i>GLC Testing in Phase 3</i>	38
5	Conclusions and Future Work	44
	References.....	45
	Appendices.....	47
	Appendix A: Pure PCM-6 Heating Test	47
	Appendix B: PCM-6 Absorption and Evaporation Tests.....	47
	Appendix C: Procedure for Mixing and Compacting Cube Samples with Mechanical Mixer.	48
	Appendix D: CoreLok Procedure for the Theoretical Maximum Density Test	49
	Appendix E: Procedure for Mixing and Compacting Cube Samples by Hand Mixing	50
	Appendix F: Bulk Specific Gravity (BSG) of Compacted Samples	51
	Appendix G: Raw Data for Absorption of PCM-6 into LWA	52
	Appendix H: Temperature Profiles for all Phase 2 GLC Trials.....	53
	Appendix I: Calculations for Theoretical Maximum Density (TMD) Test	54
	Appendix J: Volumetric Property Calculations	55

List of Figures

Figure 1: FOD sweepers commonly used at airports. ⁷	4
Figure 2: (a) Longitudinal cracking along the direction of the pavement centerline. ¹⁰ (b) Transverse cracking perpendicular to the pavement centerline. ¹⁰	6
Figure 3: Reflection cracking in an HMA overlay. ¹⁰	7
Figure 4: Rutting failure within the wheel path of an HMA pavement. ¹⁰	8
Figure 5: Latent heat versus sensible heat energy storage in a PCM. ¹⁵	10
Figure 6: Theoretical illustration of the effect of a PCM on the material temperature profile.	11
Figure 7: Schematic showing the action of repeated wheel loads over time to create rutting in HMA.	12
Figure 8: Transverse cracks caused by thermal cracking in a roadway pavement. ¹⁷	13
Figure 9: Concept graph of the relationship among tensile strength, thermal stress, and temperature in HMA. ⁹	14
Figure 10: Thermal stress gradient in an HMA layer which causes top-down cracking. ¹⁷	14
Figure 11: Diagram of the GLC device.	20
Figure 12: GLC cycle for Phase 2 thermal property testing.	21
Figure 13: GLC cycle for Phase 3 thermal property testing.	24
Figure 14: First PCM-6 evaporation test.	26
Figure 15: Second PCM-6 evaporation test.	26
Figure 16: Compacted HMA samples with 1.25% PCM-6.	27
Figure 17: Samples with 10.5% PCM-6 after demolding.	28
Figure 18: Observed difference in color shading on faces of cubes with 2.5% PCM-6.	29
Figure 19: Phase 2 heat flow versus average temperature for samples.	30

Figure 20: Average temperature versus time for sample averages.	31
Figure 21: Data from all cycles of PCM 2.5%.....	32
Figure 22: Phase 2 trial average temperature versus time.	33
Figure 23: Trial averages at approximate phase change temperature (thawing).	34
Figure 24: Plot of aggregate gradations for HMA mixes.	36
Figure 25: Phase 3 batch of 1.25% PCM-6 samples after demolding.	37
Figure 26: Phase 3 heat flow versus average temperature for samples.	39
Figure 27: Phase 3 trial average temperature versus time.	40
Figure 28: Temperature profile of sample 1 PCM 1.25% (Phase 3).	41
Figure 29: Temperature profile of sample 1 PCM 1.25% (Phase 2).	42

List of Tables

Table 1: FAA classification of airports. ¹	1
Table 2: FAA classification of general aviation airports. ³	2
Table 3: Table of pavement ratings and treatments. ¹²	9
Table 4: Summary of testing phases.	17
Table 5: Mix design for control batch.....	19
Table 6: Mix design for 1.25% PCM-6 batch.....	19
Table 7: Mix design for 10.5% PCM-6 batch.....	19
Table 8: Mix design for 5.5% PCM-6 batch.....	19
Table 9: Mix design for 2.5% PCM-6 batch.....	19
Table 10: Mix design for control batch.....	23
Table 11: Mix design for 1.25% PCM-6 batch.....	23
Table 12: Absorption test data.	25
Table 13: Maximum and average standard deviations for sample cycles (1 cycle = 3 trials).	32
Table 14: Volumetric properties of HMA samples.....	38
Table 15: Phase 3 extreme temperatures, freezing/thawing times and thermal conductivity.....	40

Glossary of Terms

AIP	Airport Improvement Program
ASTM	American Society for Testing and Materials
BSG	Bulk Specific Gravity
FAA	Federal Aviation Administration
FOD	Foreign Object Debris
GLC	Guarded Longitudinal Calorimeter
HMA	Hot Mix Asphalt
LWA	Lightweight Aggregate
MassDOT	Massachusetts Department of Transportation
Massport	Massachusetts Port Authority
NPIAS	National Plan of Integrated Airport Systems
NWA	Normal Weight Aggregate
PCC	Portland Cement Concrete
PCI	Pavement Condition Index
PCM	Phase Change Material
PEG	Polyethylene Glycol
TES	Thermal Energy Storage
TMD	Theoretical Maximum Density
VFA	Voids Filled with Asphalt
VMA	Voids in the Mineral Aggregate
VTM	Voids in the Total Mix

1 Introduction

There are currently 19,786 landing facilities across the United States that are used to support the aviation industry. Of these facilities, 26% (5,171) are open to the public while the remainder is private-use only. The main differences between public and private-use airports are that public airports, such as JFK International (NY), are eligible for federal funding while private-use airports, such as Ware Airport (MA), are ineligible for funding and require the permission of the owner for use. Private-use airports also include military bases. Of the 5,171 public-use airports, 3,300 are considered national assets under the National Plan of Integrated Airport Systems (NPIAS).

Table 1: FAA classification of airports.¹

Airport Classifications		Hub Type: Percentage of Annual Passenger Boardings	Common Name
Commercial Service: Publicly owned airports that have <u>at least 2,500</u> passenger boardings each calendar year and receive scheduled passenger service §47102(7)	Primary: Have <u>more than 10,000</u> passenger boardings each year §47102(11)	Large: 1% or more	Large Hub
		Medium: At least 0.25%, but less than 1%	Medium Hub
		Small: At least 0.05%, but less than 0.25%	Small Hub
	Nonprimary	Nonhub: More than 10,000, but less than 0.05%	Nonhub Primary
Nonprimary (Except Commercial Service)	Nonhub: At least 2,500 and no more than 10,000	Nonprimary Commercial Service	
		Not Applicable	Reliever §47102(18)

Airports that are considered national assets are those that are significant to the national air transportation infrastructure and, if eligible, can receive federal grants under the Airport Improvement Program (AIP) for planning and development.² The remaining 1,841 public-use airports are not included in the NPIAS if they are located at inadequate sites, cannot be expanded and improved to provide a safe and efficient airport, or are located within 20 miles of another

NPIAS airport.² The breakdown of airports is strictly defined by the Federal Aviation Administration (FAA), which helps accurately determine the types and sizes of runways in the United States (Table 1).²

Commercial airports are one of the broader categories of airports and include regularly scheduled flights. These airports are publicly owned and have at least 2,500 passenger enplanements (boardings) annually. The airports are then sub-divided into hub sizes, which are determined based on amount of enplanements and percentage of enplanements with respect to total enplanements in the U.S. In total, there are 29 airports in the U.S. defined as large hubs, such as General Edward Lawrence Logan International (MA), which together account for 70% of total annual enplanements. The medium (36) and small (74) hub airports account for 27% of total annual enplanements. Together, these 139 airports, which represent less than 1% of all airports in the US, account for 97% of the total annual enplanements.²

Another important aspect of the aviation industry is general aviation. General aviation is associated with civilian services and includes, but is not limited to: aeromedical flights, emergency responses, taxi services, corporate flights, recreational flying, research, moving cargo, general delivery services and much more.^{2,3} Currently, 2,952 of the airports under NPIAS are considered general aviation.² General aviation airports include privately-owned, public use airports that enplane 2,500 or more passengers annually and receive scheduled airline service. The classification of general airports was broader, but in 2012 the FAA further classified these airports and successfully sub-categorized 2,455 of the 2,952 airports (Table 2).

Table 2: FAA classification of general aviation airports.³

National (84)	Regional (467)	Local (1,236)	Basic (668)
Supports the national and state system by providing communities with access to national and international markets in multiple states and throughout the United States.	Supports regional economies by connecting communities to statewide and interstate markets.	Supplements local communities by providing access primarily to intrastate and some interstate markets.	Supports general aviation activities such as emergency service, charter or critical passenger service, cargo operations, flight training, and personal flying.

In addition, these airports include reliever airports. Reliever airports, which may be publically- or privately-owned, were initially designated to relieve congestion at commercial service airports, but now many serve their own economic and operational role.³ The reliever airport is just one

example of how general aviation has evolved to support a diverse range of needs. Although varying in size and facilities, general aviation airports provide important connections to the larger aviation network and provide services for the communities in which they are located. These airports are covered by NPIAS because they support commerce, help connect the U.S. aviation network, as well as provide a safety net for aircraft in case of mechanical problems, medical emergencies, deteriorating weather conditions or other unforeseen circumstances.³

Having well-maintained and safe runways is pivotal in ensuring the ability of the aviation industry to function safely and economically. To maintain the quality of the aviation infrastructure, the FAA currently aims to keep 93% of public-use runways at excellent, good, or fair condition.² Keeping a runway, whether large or small, in operation is crucial in ensuring timely service and safe operating conditions for aircraft.² The purpose of this project was to explore the feasibility of incorporating phase change materials (PCMs) into hot mix asphalt (HMA) as a method for reducing damage from thermal stresses in airport pavements. The incorporation of PCM was expected to improve safety by reducing debris from deteriorating pavement, therefore decreasing the amount of time, money and resources necessary to maintain runway pavements.

2 Background

2.1 Foreign Object Debris (FOD)

One of the major safety concerns of airports is the accumulation of foreign object debris (FOD) on runways and taxiways. The debris consists of unwanted items, such as stones, items that have fallen from planes, baggage pieces, and trash. Every year, FOD at airports causes \$12 billion of damage to airplanes and airport infrastructure.⁴ A particularly important issue is the danger that debris poses to airport personnel and passengers. In 2000, all 109 passengers and crew and four people on the ground were killed when Air France Flight 4590 crashed due to FOD.⁵ In this particular instance, a small piece of metal from a previous plane cut the tire of Flight 4590 despite the debris being on the runway for less than five minutes.

FOD is removed in various ways depending on the amount and location of the debris. The most common way to remove large amounts of debris from open areas such as runways is to use a FOD sweeper. The FOD sweeper is dragged by a vehicle and forces the small objects into holding sections that are emptied after every few miles of sweeping (Figure 1). Another device is the motor powered vacuum, which is ideal for smaller areas where a FOD sweeper cannot be towed by a vehicle. Other methods include rumble strips which free any debris from an airplane during taxiing. The rumble strips are grooves cut into the pavement and are designed to shake the plane just enough to dislodge any debris clinging to the exterior. Removal of FOD is an important task to ensure safety.⁶



Figure 1: FOD sweepers commonly used at airports.⁷

2.2 Properties of Hot Mix Asphalt (HMA)

Hot mix asphalt (HMA) is a widely used material for roadways and airport pavements. Where environmental factors allow the use of an asphalt material, it serves as a cheaper alternative to portland cement concrete (PCC) pavements. Generally, asphalt pavements are used

in cooler regions because high temperatures will damage asphalt pavements over time. However, the choice between an asphalt and concrete pavement also depends on economics and the policies present in the region. Besides these factors in selecting a pavement type, there are significant differences in the material properties of HMA and PCC that must be taken into account. The strength of a flexible HMA pavement is often lower than its rigid PCC counterpart due to the different load resistance mechanisms employed by the two pavement types.⁸ HMA pavements are viscoelastic materials, which means they behave as a viscous fluid, elastic solid, or a combination of the two, depending on temperature and loading duration. The viscoelastic nature of HMA is due to the use of bitumen, a semi-solid form of petroleum, as the asphalt binding agent. The asphalt binder, and consequently the modulus of elasticity of the pavement, is greatly affected by both the temperature and the loading time, which depends on the speed of the vehicle.⁹

The temperature of the pavement affects how the material will behave mechanically. At high temperatures, the asphalt binder behaves more like a fluid and loses its ability to hold the constituent parts of the pavement together in a solid mass. The pavement then acts as a viscous material, which causes a decrease in the modulus of the HMA layer, resulting in a lower overall strength and stiffness.⁹ As loads are applied to the structure, it will deform plastically until it reaches a terminal serviceability, and is no longer suitable for vehicular travel. On the other hand, lowering the temperature of the pavement causes the asphalt binder to behave more like an elastic solid with a much higher modulus and strength and a significantly increased resistance to flow. When loads are applied to a pavement under these conditions, the pavement can support the load and will only experience elastic deformation. Thus, after the load is removed the pavement will return to its original state. This cycling persists for as long as loading repetitions are kept within the allowable maximum load and number of load cycles for which the pavement was designed.⁹

Another major factor affecting the performance of HMA is the loading period. Since asphalt binder is a viscoelastic material, changing the rate of loading produces different responses from the pavement. A load applied and removed over a short duration will generate an elastic response from the pavement structure.⁹ This response is analogous to a truck or aircraft riding at a high speed over a section of pavement. However, if a load is applied to a pavement continuously over a long period of time, the pavement will behave as a viscous fluid. Gradually,

the structure will deform plastically under the load, and when the load is released the structure will remain deformed.⁹

In the case of airports, the high-speed, short-term loading during takeoff and landing creates a more elastic response. Mid- and long-term loading occurs on taxiways where planes travel at lower speeds, and occasionally come to a stop as they form queues for takeoff. Lastly, parking aprons are the longest-term loading case because aircraft remain at rest for long periods for fueling, boarding, maintenance, and other activities. This long loading period creates the greatest viscous response from the pavement.

2.3 Pavement Distresses

Various problems can arise within flexible pavement systems, such as cracking, disintegration, distortion, and loss of friction. Cracking can be in the longitudinal and/or transverse direction. Longitudinal cracks (Figure 2a) are typically due to fatigue of the pavement by repeated loading, while transverse cracks (Figure 2b) are often fractures in the pavement caused by thermal fluctuations, or a combination of thermal vehicular stress. A decrease in pavement temperature causes an increase in stiffness while the pavement tries to contract due to the change in temperature. However, the pavement is restrained from contracting due to frictional bonds with the layers beneath it. The resulting tensile stresses in the pavement may exceed the tensile strength of the material and result in the formation of transverse cracks.

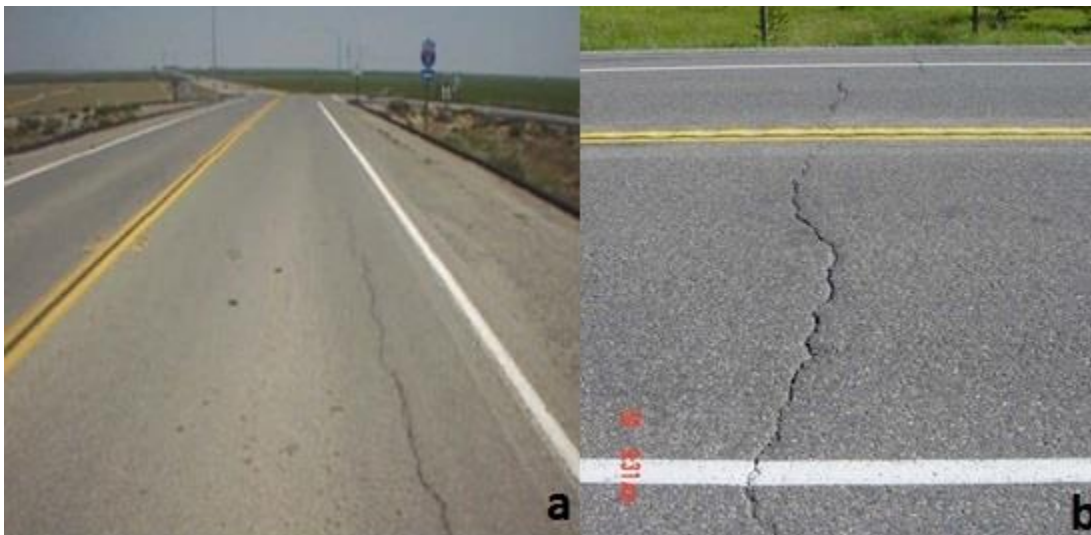


Figure 2: (a) Longitudinal cracking along the direction of the pavement centerline.¹⁰ (b) Transverse cracking perpendicular to the pavement centerline.¹⁰

Over time, longitudinal and transverse cracks will intersect and form block cracks, which are rectangular sections of pavement that spall and disintegrate under environmental conditions

and traffic loads. These cracks may lead to the separation of loose pieces or particles and resultant FOD.⁸ In certain pavements, reflection cracking may also result from thermal expansion and contraction (Figure 3). These cracks occur where a pavement layer with existing cracks (or a PCC layer with joints) is overlaid by a layer of HMA. As the lower layer continues to experience thermal stresses, it will cause the same pattern of cracking to form in the top layer of pavement.⁸ If these cracks exist for an extended period of time, water will infiltrate the pavement structure. The presence of water will deteriorate the pavement further through freeze-thaw cycling and/or the stripping of asphalt from aggregates. In airports, this degradation will quickly result in a significant FOD hazard to aircraft due to raveling and weathering of the weakened surface.¹¹



Figure 3: Reflection cracking in an HMA overlay.¹⁰

The second category of flexible pavement distress is disintegration. The most notable product of disintegration is the formation of potholes. Potholes often result from fatigue or alligator cracking, which is not a thermal issue. However, water infiltration and freeze-thaw cycling in cold areas, such as New England, can cause a rapid growth in pothole severity, whether the pothole began due to thermal- or fatigue-cracking phenomena.⁸ Patches from previous repair jobs also serve as potential freeze-thaw sites where disintegration can occur. A more unique type of pavement disintegration for airports is jet blast erosion, which occurs when the binder in the pavement surface (0-0.5 in or 0-1.27 cm in depth) is burned or carbonized.⁸ Jet blast erosion is not an environmental thermal issue in the pavement, but rather a thermal condition to which the pavement is exposed during service. These types of deterioration can lead to loose aggregate material on the surface which creates FOD on the runway.

The third class of distress is distortion, or displacement of the pavement surface. Rutting (Figure 4) is the most common form of distortion and results from permanent deformations in

any of the pavement layers or the subgrade. If the subgrade is deformed, the rutting is often due to incorrect structural design. However, if rutting occurs in the HMA surface layer, this could be due to several different factors. From a thermal perspective, asphalt mix modulus decreases with an increase in temperature, resulting in lowered pavement stiffness. This softening allows the pavement to gradually consolidate or deform in plastic mode under applied loads. Deformations resulting from this type of failure include general rutting, corrugation (surface ripples), shoving, or local depressions. These distresses directly affect aircraft movement through a greater potential of hydroplaning and FOD hazards.¹¹



Figure 4: Rutting failure within the wheel path of an HMA pavement.¹⁰

The final class of HMA pavement distress is loss of friction. This category often does not involve problems caused by a thermal factor, except in the case of bleeding. Bleeding occurs during hot weather when asphalt binder expands to fill the air voids in a pavement and then moves to the surface, creating a thin film over the pavement. Often this distress is caused by a combination of poor mix design, poor construction, and hot weather conditions, and it can result in an increased chance of skidding.¹¹

2.4 Pavement Treatments

Airports utilize a number of treatments in order to maintain airport pavements. For example, cracks can be filled with sealants in order to prevent freeze-thaw deterioration and spalling. Similarly, small area patching can repair potholes and/or alligator cracking. In addition, spray patching with a manual chipseal or a mechanized spray can block cracking, rutting, frost heave, and subgrade settlement. Rejuvenators and seals can fill the asphalt surface, as well as rejuvenate oxidized or hardened binder.⁸ This method can also protect binder from being dissolved in future fuel spills or oil leaks by creating a protective barrier. Texturization using fine

milling or controlled shot-blasting can condition pavement smoothness and improve friction to prevent rutting, bumps, and other distress. Surface treatments can repair minor cracks, raveling, and restore surface friction. Furthermore, slurry seal can be used to improve distresses on the asphalt surface, such as raveling, loss of coarse aggregate, and seal cracking, in addition to waterproofing and improving surface friction.⁸ Overall, the method of treatment or solution depends on the type of distress observed, the maintenance plan, and the budget of the airport.

2.5 Airport Pavement Maintenance

The maintenance policy used for cracking depends on the severity of the cracking observed as well as the cost of treatment options. As shown in Table 3, one method for measuring cracking is the Pavement Condition Index (PCI). If a crack is not very severe, no maintenance treatment is carried out, but the distress should be monitored. If a crack has medium severity then it is routed and sealed to repair the damage and prevent further distress. If a crack is considered high severity, then crack repairs are carried out.¹²

Table 3: Table of pavement ratings and treatments.¹²

PCI Rating	Description	Treatments
86 - 100	Good — only minor distresses	Routine Maintenance
71 - 85	Satisfactory — low and medium distresses	Preventive Maintenance
56 - 70	Fair — some distresses are severe	Corrective maintenance and rehabilitation
41 - 55	Poor — severity of some distress can cause operational problems	Rehabilitation or reconstruction
26 - 40	Very Poor — severe distresses caused operational problems	Rehabilitation and reconstruction
11 - 25	Serious — many severe distresses operational restrictions	Immediate repairs and reconstruction
0 - 10	Failed — pavement deterioration prevents safe aircraft operations	Reconstruction

The cost of maintenance to keep airport pavements safe is substantial. The Federal Aviation Administration (FAA) estimates that between 2013 and 2017, there will be \$42.5 billion worth of Airport Improvement Program (AIP) eligible infrastructure projects.² Also, rehabilitating pavements in poor condition may cost two to three times more than rehabilitating pavements in good condition because the methods needed to restore severely deteriorated pavements are significantly more expensive.¹³ Thus, it is crucial to not allow pavements to reach a point where costly solutions are the only option.

2.6 Phase Change Materials (PCMs)

In order to minimize the cost associated with the maintenance of airport pavements, performance of a pavement exposed to environmental factors should be improved. Temperature is one of the most important environmental factors affecting this performance, since large temperature changes have the potential to cause significant damage to pavements. Significant improvement in performance, and therefore reduction in maintenance costs, may be possible if the magnitude of these changes in temperature could be decreased. One method that may be able to accomplish this is incorporating phase change materials (PCMs) into a pavement mix.

Construction and other commercial industries use PCMs as thermal energy storage (TES) systems. In the past, TES systems have used materials with significant sensible heat storage. In other words, these materials have heat storage abilities that occur during a change in temperature, but do not require a change in phase. As research into this technology has progressed, materials have been identified which can store more energy as latent heat than previous sensible heat storage materials. PCMs are materials with a high latent heat of fusion (ΔH_f°) which allows large amounts of heat to be absorbed or released during a phase change (Figure 5).¹⁴ There are many families of PCM compounds, each with a range of melting points, which allows for a wide range of applications. Some families of PCMs include organic compounds, such as polyethylene glycol (PEG); saturated hydrocarbons, such as paraffin waxes; inorganic salts and salt hydrates; and eutectic solutions of salts and salt hydrates.¹⁵

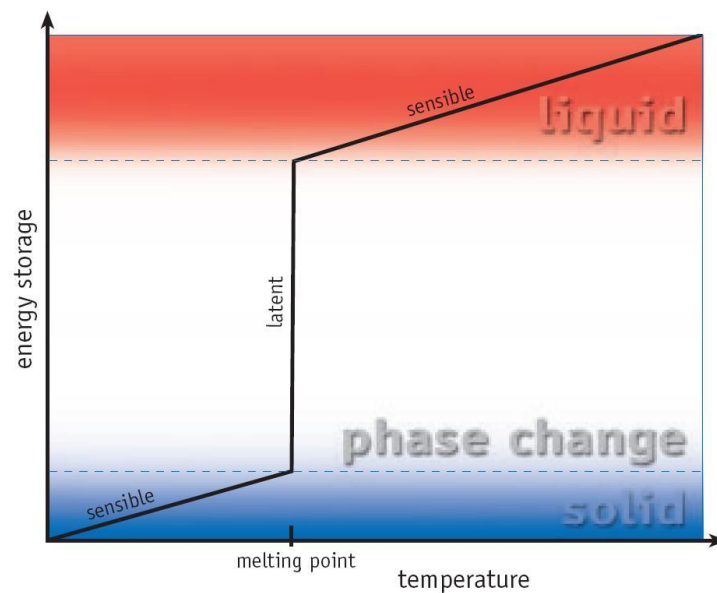


Figure 5: Latent heat versus sensible heat energy storage in a PCM.¹⁵

PCMs are temperature regulating materials that have the ability to release or absorb heat. The release or absorption of heat occurs during the phase change, which makes the proper selection of a PCM largely dependent on the temperature at which the phase change occurs. For example, PCM-6 (a blend of paraffin waxes), is liquid at room temperature, but as the system temperature lowers to 6 °C (the phase change temperature), the material undergoes an exothermic phase change and solidifies. Conversely, when the system warms, the phase change material undergoes an endothermic reaction and liquefies. Although relatively large amounts of heat are either released or absorbed during these transition periods, the temperature of the surrounding environment remains at the phase change temperature of the PCM. The time during which the temperature remains at this value depends on the value of the latent heat of fusion of the PCM, which means that materials with a high latent heat of fusion can delay a temperature change in their environment for a longer period of time (Figure 6).

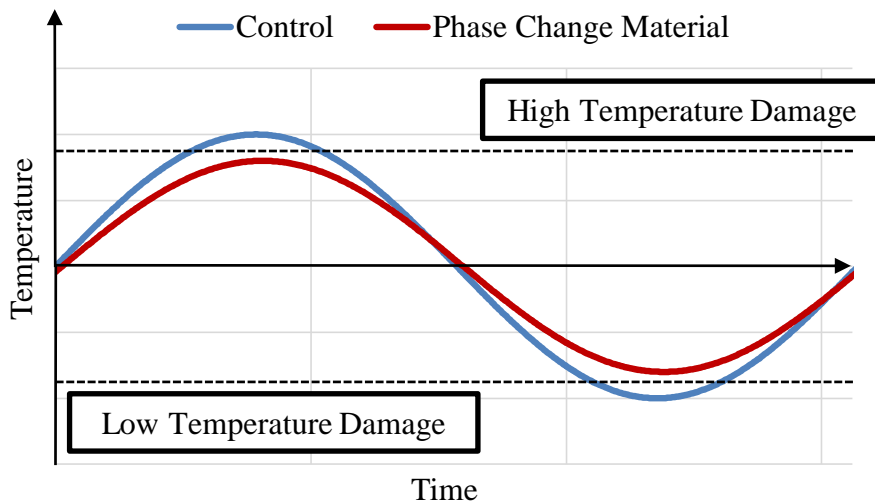


Figure 6: Theoretical illustration of the effect of a PCM on the material temperature profile.

2.7 Rutting and Thermal Cracking in HMA

The properties of PCMs can theoretically be applied to mitigate rutting and thermal cracking in HMA, assuming a proper mix design with adequate strength and other properties can be achieved. Rutting in the HMA can be due to vertical deformations caused by local increases in density when large loads traverse a pavement with a hot surface temperature. The high temperature allows the mix to compress to a state with lower air voids under this extreme condition.⁹ A more typical occurrence is deformation or movement of the pavement in both the vertical and horizontal directions due to a shear failure in the pavement. Shear failure occurs

when pavements exposed to high temperatures and repeated loads over time lose their binding strength and begin to deform plastically. These deformations often involve a vertical displacement of material under the wheel path, which in turn causes nearby sections of the pavement to move laterally or rise, producing ripples or channels in the pavement surface (Figure 7).⁹

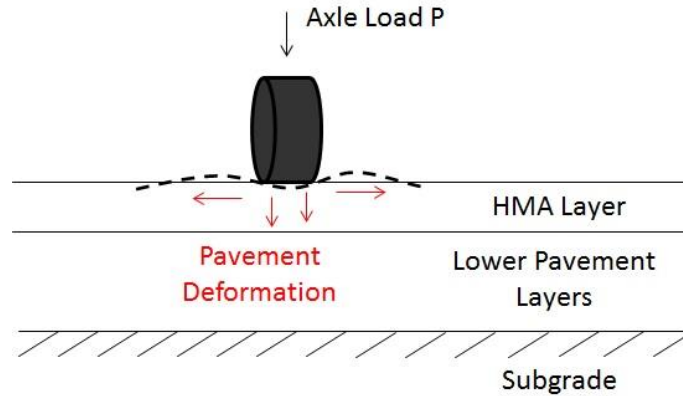


Figure 7: Schematic showing the action of repeated wheel loads over time to create rutting in HMA.

General models to determine rutting in the HMA layer involve the calculation of the vertical plastic strain that the layer undergoes, as stated in the following set of equations:¹⁶

$$\frac{\varepsilon_p}{\varepsilon_r} = k_1 * a * N^b * T^c \quad (1)$$

$$RD_{HMA} = \varepsilon_p * h_{AC} \quad (2)$$

In Equations 1 and 2, the plastic strain fraction ($\varepsilon_p/\varepsilon_r$) is calculated using the total number of loads (N), the pavement temperature (T, °F), and a non-dimensional depth correction factor (k_1). The data are correlated using several experimental coefficients (a, b, and c), and the total rutting (RD_{HMA} , in) is found by multiplying the plastic strain by the thickness of the HMA layer (h_{AC} , in). The depth correction factor is found using the following experimentally determined equations which are a function of HMA thickness (h_{AC} , in) and depth to computational point (depth, in):¹⁶

$$k_1 = (C_1 + C_2 * depth) * 0.328196^{depth} \quad (3)$$

$$C_1 = -0.1039 * h_{AC}^2 + 2.4868 * h_{AC} - 17.342 \quad (4)$$

$$C_2 = 0.0172 * h_{AC}^2 - 1.7331 * h_{AC} + 27.428 \quad (5)$$

PCM may be a viable method to reduce the potential for rutting of asphalt pavements in hot climates. For this scenario, a PCM with a melting point significantly above room temperature (70 °F or 20 °C) would be selected and incorporated into the HMA mix design. As the temperature rises, the PCM would melt and absorb heat, thus cooling the overall system.¹⁴ By doing so this would lower the overall temperature values used in Equation 1, thus decreasing the rutting in the HMA layer.

The other distress mechanism which PCMs may be able to reduce is thermal cracking. Thermal cracking can occur as either low-temperature cracking or thermal fatigue cracking (Figure 8). In low-temperature cracking, the pavement is exposed to extreme low temperatures which cause the pavement to want to contract. However, the pavement is constrained by the base layer in all directions, and it is also constrained in the longitudinal direction by the continuous layer of mix which makes up the lane. High longitudinal stresses build up at the surface of the pavement where the temperature is lowest, and decrease in magnitude within the pavement cross-section.



Figure 8: Transverse cracks caused by thermal cracking in a roadway pavement.¹⁷

Due to the viscoelastic nature of hot mix asphalt, the initial cooling of the pavement results in a temporary increase in the tensile strength of the HMA (Figure 9). However, once the tensile stresses in the pavement become large, microcracks begin to form and cause local decreases in tensile strength. These cracks form from the surface down because the temperature change is greatest at the surface of the pavement, producing a stress distribution conducive to crack propagation (Figure 10). Some microcracking can heal if the pavement returns to a viscous temperature, but crack propagation and expansion will continue to damage the pavement if temperatures remain low enough to cause continued high tensile stress in the pavement.

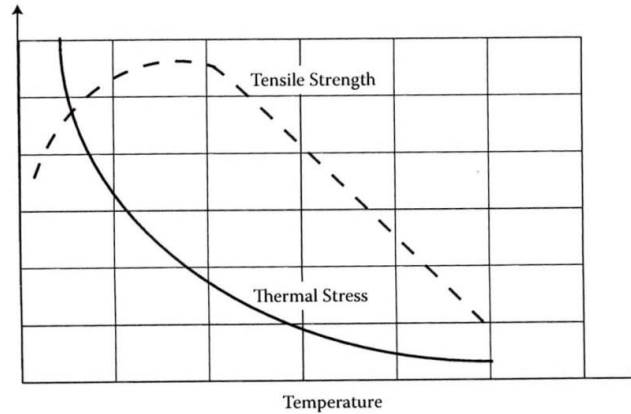


Figure 9: Concept graph of the relationship among tensile strength, thermal stress, and temperature in HMA.⁹

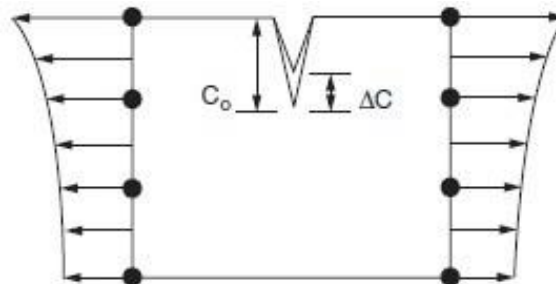


Figure 10: Thermal stress gradient in an HMA layer which causes top-down cracking.¹⁷

If temperatures remain such that low-temperature cracking does not occur because the tensile strength is not exceeded, the HMA will not fail immediately. However, strains may build up after repeated high- and low-stress cycles produced by temperature fluctuations and traffic loading over time. This could lead to failure in the long term by thermal fatigue cracking.⁹ These repeated stress cycles are often inevitable over the lifetime of a pavement. PCMs may be able to reduce a pavement's susceptibility to thermal fatigue cracking. As the temperature of the pavement decreases, the PCM will freeze and release heat into the matrix keeping the system warmer than the surrounding ambient temperature.¹⁸ If a pavement contained a PCM with a low enough melting point, the PCM could temporarily prevent the pavement from crossing or approaching the operational threshold of the binder, depending on the frequency and intensity of low-temperature cycles. In this way the PCM can reduce the extremes of temperature fluctuation and make pavement temperature profiles smoother. This smoother profile may also help to deter freeze-thaw cycling in pavements which have absorbed water. A PCM appropriate for this purpose would need a phase change temperature above the freezing point of water.

3 Methodology

3.1 Evaluation of Facility Problems and Definition of Project Scope

In order to gain specific information on common types of thermal damages to airport pavements, professionals with knowledge of airport pavements were contacted. Questions were geared to each recipient's location and areas of expertise, and were developed in order to gain a range of information. The respondents included John Kirkendall (Jacobs Engineering), Jonathan Neeser (Worcester Airport), and Barry Hammer (FAA Airports Division).

John Kirkendall of Jacobs Engineering responded that he has seen firsthand the effects of thermal distresses at airports in Alaska. He identified frost heave and potholes as the most predominant problems facing airports in that region. According to Mr. Kirkendall, one of the most important ways to prevent airport pavement damage is to repair and prevent cracking, which can allow water to penetrate the asphalt and cause even more damage. Airports in the region use HMA more often than PCC mostly because of the shorter construction time associated with HMA.

Jonathan Neeser of the Worcester Airport stated that although asphalt deterioration does cause FOD at the airport, this is mainly caused by segregation of the HMA and not by thermal distresses. He believes that thermal distresses of the pavements are not predominant at the airport because of the quality of the system used, including proper drainage, and quality mix design and materials. The majority of the damage to the airport pavements is seen near the airplane hangars and not on the runway itself. The HMA at the Worcester Airport is tested for acceptable ranges of stability, flow, air voids, and density.

Barry Hammer with the FAA Airports Division confirmed the importance of FOD safety by noting how loose aggregate, even in the form of a small stone, could have devastating effects if it entered a jet engine intake. He also explained that the most severe freeze-thaw impacts are at airports constructed on frost-susceptible materials, such as clay and silt. However, Mr. Hammer also noted that the conventional wisdom in regards to freeze-thaw is that the adverse impacts of freeze-thaw cycling were a result of this action in the base materials, not within the pavement material itself. "Usually cracks open up, allow water to penetrate into the base materials and if the water becomes trapped because the materials are frost-susceptible we see traditional heaving action which further deteriorates the pavement," he explained.

The results of these professional contacts indicate that water penetration of HMA

pavements through surface cracks has traditionally been a cause for concern because it allows for pavement deterioration by a variety of failure modes. Specifically, freezing of this water within pavement layers is a concern for airport pavement maintenance. If crack initiation at the surface could be reduced, then this will reduce the total number of entry points for water to enter the pavement. This reduction of entry points will correspond to a reduction in stripping, raveling, cracking, and pothole formation, which will lead to lowered overall maintenance costs for airports. In order to identify possible solutions for surface crack reduction, it was decided to investigate the feasibility of incorporating low-temperature PCM into HMA.

3.2 Experimental Methods Summary

Before attempting to incorporate PCM-6 into HMA, uncertainties with the behavior of the PCM-6 were investigated. First, a beaker containing 20 mL of PCM-6 was placed in an oven at 150 °C to simulate the conditions of mixing HMA in order to determine if the material would ignite (Phase 1). After determining that the material would not ignite, absorption, and evaporation tests were conducted to determine how much PCM-6 was absorbed by the lightweight aggregate (LWA) and how much evaporated during the HMA mixing process. Test cubes were then constructed to assess the feasibility of using LWA as a method for incorporating PCM-6 into HMA. Then, the thermal properties of the samples were evaluated using a Guarded Longitudinal Calorimeter (GLC) to determine the thermal impacts of incorporating PCM-6 into HMA (Phase 2). To address the issues with incorporating PCM-6 into test cubes, iterations of mix designs were performed to determine the threshold amount of PCM-6 that could be incorporated without significant loss of material strength. After selecting a final mix design, a final batch of samples was produced and subjected to theoretical maximum density tests, specific gravity tests, and an improved GLC test procedure (Phase 3). The Superpave specification was used throughout the project.¹⁹ The different phases, tests and dimensions/amounts of test specimens are summarized in Table 4.

Table 4: Summary of testing phases.

Phase	Test	Dimensions/Amount
Phase 1 – Absorption and Evaporation Tests		
1	PCM-6 Heating Test	20 mL
	Absorption/Evaporation Test	-
Phase 2 – Feasibility of a HMA/PCM Mix		
2	GLC Testing	2"x2"x2"
	Control	
	1.25% PCM-6	
	2.5% PCM-6	
Phase 3 - Improved Mix Design		
3a	GLC Testing	2"x2"x2"
	Control	
	1.25% PCM-6	
3b	Theoretical Maximum Density	2"x2"x2"
	Control	
	1.25% PCM-6	
3c	Bulk Specific Gravity	2"x2"x2"
	Control	
	1.25% PCM-6	

3.3 Phase 1: Heating and Evaporation Tests

Before experimenting with incorporating PCM-6 into HMA, an evaporation test was conducted to determine how liquid PCM-6 would behave in conditions similar to those involved in the preparation of HMA. The purposes of this experiment were to investigate whether the material would ignite at high temperatures and to calculate the evaporation rate of liquid PCM-6. To conduct the test, a beaker with 20 mL of PCM-6 was placed in an oven at 150 °C for 1 hour and monitored for combustion. Upon completion, it was determined that the PCM-6 was non-combustible at 150 °C and the final amount of PCM-6 was measured to estimate loss due to evaporation. The full experimental procedures can be found in Appendix A.

After determining that the PCM-6 was safe for mixing, a series of trials were conducted to determine the amount of PCM-6 that would be absorbed by the LWA and the evaporation rate during heating. Three trials of four combinations (12 samples) of LWA were tested: No. 4 sieve, No. 8 sieve, No. 16 sieve, and an equal mixture of each of the aforementioned sieves. The LWA was soaked in PCM-6 for 24 hours before being placed in the oven at 150 °C for 3 hours. After

every 30 minutes the amount of PCM-6 was measured and recorded. Since it was found that the PCM-6 evaporated quickly, a second test requiring 12 new samples was conducted for 30 minutes with weights measured at 5-minute intervals. The full experimental procedures can be found in Appendix B.

3.4 Phase 2: Sample Production and Thermal Testing

After investigating the properties of PCM-6, it was possible to begin producing test samples. These samples were designed to act as conceptual samples to determine the feasibility of incorporating PCM-6 into HMA. The samples contained aggregate retained on sieve sizes No. 4 through pan. For these samples, 20% of the aggregate was from a natural sand stockpile and the remaining 80% from a crushed stone stockpile. Since proportions of individual sieve sizes were not used, an initial binder content of 5.5% was increased to 9% by mass to account for excess fines in the mix, which absorb asphalt binder. The mix design began with a volume of aggregate approximately equal to 8 in³ (131 cm³) and a corresponding mass of binder based on the binder content. The PCM-6 was incorporated via absorption into the LWA, which replaces an equivalent volume of normal weight aggregate (NWA) in the mix. A threshold value of 10% LWA by mass was used as an estimate for the maximum amount that could be added before the mechanical properties of the HMA would be adversely affected. To calculate the amount of PCM-6 to add to each sample, the water absorption of LWA was used to back-calculate the theoretical PCM-6 absorption of LWA. This calculated value of 13.3% by mass, which was supported by the absorption test data, was used to batch the amount of PCM-6 and LWA needed for any given batch of samples.

3.4.1 Sample Production

Using the results from the PCM-6 absorption and evaporation tests, a mixing procedure was designed and utilized to construct 2 in (50 mm) cube samples. Exact PCM contents were calculated for each mix design, but due to losses during the heating and mixing process, approximate target contents are used to identify each mix design. The target concentrations were 0% (control), 1.25%, 2.5%, 5.5% and 10.5% PCM-6 by mass. For the PCM-6 batches, the theoretical amount of absorbable PCM-6 and the LWA were placed in a closed container and agitated every 6 hours over a 24-hour period. The full procedure for the mixing and compaction of these samples are found in Appendix C. Table 5 through Table 9 specifies the proportions used to produce each of these batches.

Table 5: Mix design for control batch.

Mix Component	Mass (g)
Aggregate (NWA)	699
Crushed Stone	556
Natural Sand	143
Binder	73

Table 6: Mix design for 1.25% PCM-6 batch.

Mix Component	Mass (g)
NWA	894
Crushed Stone	715
Natural Sand	179
LWA	105
No. 4	21
No. 8	42
No. 16	42
PCM-6	14
Binder	95

Table 8: Mix design for 5.5% PCM-6 batch.

Mix Component	Mass (g)
NWA	427
Crushed Stone	342
Natural Sand	85
LWA	420
No. 4	84
No. 8	168
No. 16	168
PCM-6	56
Binder	95

Table 7: Mix design for 10.5% PCM-6 batch.

Mix Component	Mass (g)
NWA	0
Crushed Stone	0
Natural Sand	0
LWA	716
No. 4	143
No. 8	287
No. 16	286
PCM-6	95
Binder	64

Table 9: Mix design for 2.5% PCM-6 batch.

Mix Component	Mass (g)
NWA	633
Crushed Stone	506
Natural Sand	127
LWA	180
No. 4	90
No. 8	90
PCM-6	24
Binder	81

3.4.2 Guarded Longitudinal Calorimeter

The Guarded Longitudinal Calorimeter (GLC) consisted of an insulated cold plate that was used to generate a fluctuating or constant uniaxial heat flow through a sample of material (Figure 11). To measure the heat flow, the sample was placed inside the insulation, which has an opening of 4 in² (25.8 cm²), and six 16-gauge type K thermocouples measured the temperatures within the device. The sample was placed between two glass-ceramic blocks (2 in x 2 in x 1 in)

(5.08 cm x 5.08 cm x 2.54 cm) and the thermocouples were held in contact using 1/8 in (0.318 cm) of a thermal transfer media.

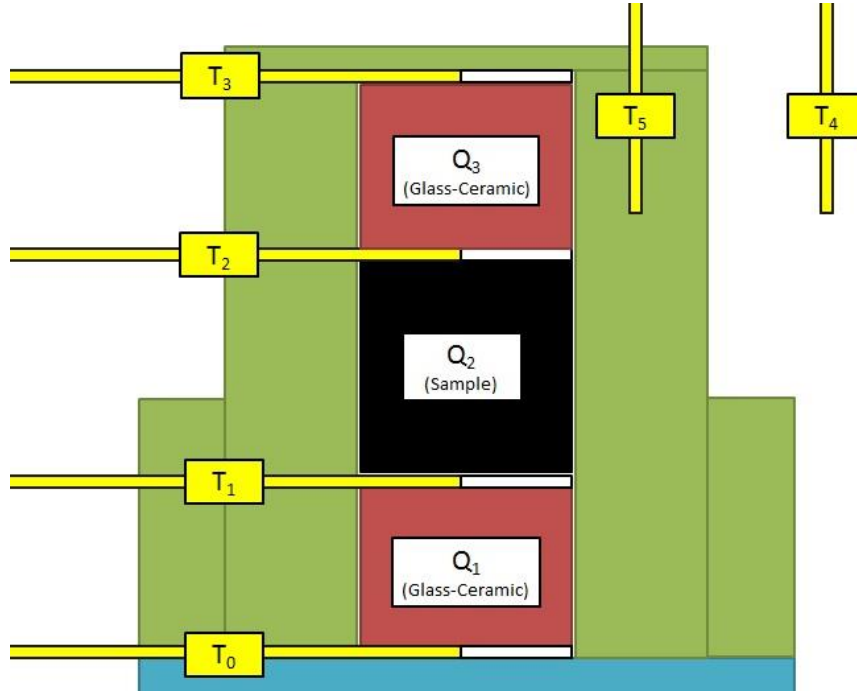


Figure 11: Diagram of the GLC device.

In total, six temperatures were recorded by a data acquisition box and four (T_0 , T_1 , T_2 and T_3) were used for estimating the heat flow. Temperature T_0 is measured at the boundary between the cold plate and a glass-ceramic block, T_1 at the boundary between one of the glass-ceramic blocks and the sample, T_2 at the boundary between the sample and the other glass-ceramic block, and T_3 at the boundary between the glass-ceramic block and the cover of the GLC. Temperature T_4 is the temperature of the ambient air and T_5 is the temperature inside the insulation. To compute the heat flow across the samples, the steady-state conduction equation given in ASTM E1225-9 was utilized, as follows:

$$Q = A_{surface} \cdot \lambda \left(\frac{\Delta T}{\Delta z} \right) \quad (6)$$

where Q (W) is the heat flow across the sample, $A_{surface}$ (m^2) is the surface area measured in the x-y plane, λ is the thermal conductivity (W/mK) of the sample, and $\Delta T/\Delta z$ (K/m) is the temperature gradient. The temperature gradient is defined as $T_n - T_{n+1}$, which implies heat flow leaving the sample is positive, and Δz , which is the thickness of the block in the z-direction, was

measured experimentally for each sample. For the known glass-ceramics, a thermal conductivity of 4.18 W/mK and Δz of 1 in (2.54 cm) was used. Because the thermal conductivity of the sample was unknown, the heat flow across the sample (Q_2) was found using the following equation:

$$Q_2 = \frac{Q_1 + Q_3}{2} \quad (7)$$

In order to apply the aforementioned heat transfer equations, it was assumed the heat flow acted only in the z-direction, conduction was the only form of heat transfer, and that the change in temperature was gradual enough to assume steady-state conditions.

3.4.3 GLC Testing in Phase 2

Phase 2 was comprised of testing three samples containing 1.25% of PCM-6, three samples with 2.5% PCM-6, and two control samples. Only two controls were constructed due to a miscalculation of the amount of material required for three and Control 2 was evaluated twice to compensate. The GLC subjected each sample to three cycles of temperatures ranging from 23 to -25 °C (Figure 12).

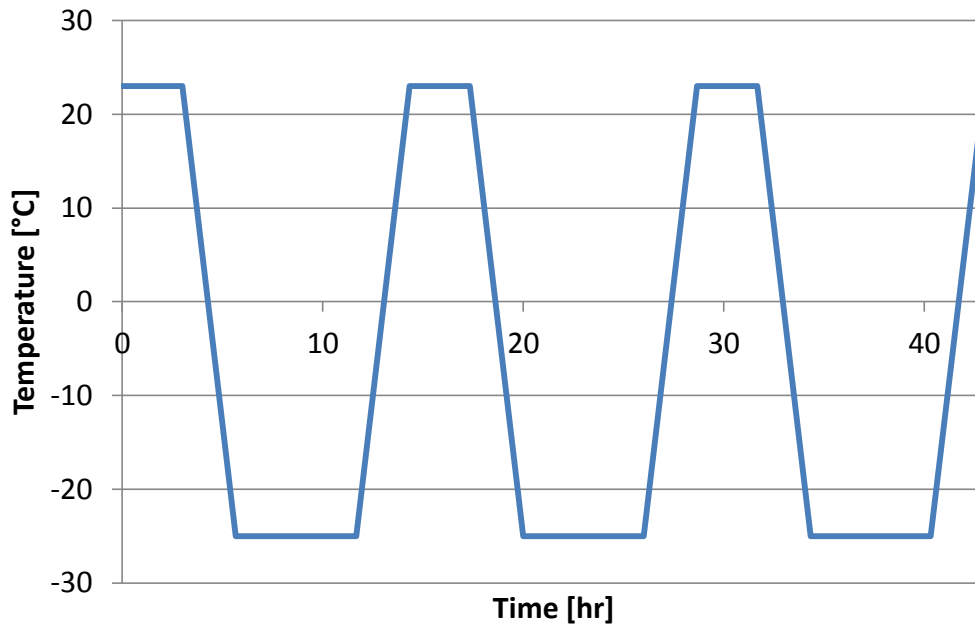


Figure 12: GLC cycle for Phase 2 thermal property testing.

The gradual changes in temperature were used to investigate whether a noticeable change in energy occurred at the phase change temperature (6 °C) for PCM-6. In addition, the

temperature plateaus (at 23 °C and -25 °C) were used to determine if the PCM minimized the extreme cold and hot temperatures. The rate of change of the temperature was programmed as 0.3 °C/min.

3.5 Phase 3: Improved Mix Design with Volumetric and Thermal Testing

After establishing the feasibility of incorporating PCM in an HMA mix, tests were performed to evaluate whether an HMA mix utilizing Superpave specifications for airfield pavements could be produced with an HMA/PCM-6 mix. A gradation analysis was performed on the aggregate stockpiles and a gradation was selected that was within the specified limits of the Superpave specification. A binder content of 5.5% was used. Theoretical maximum density (TMD) tests were conducted on the mix in order to determine the maximum density of the sample. The TMD of a mix including 1.25% PCM-6 in LWA was back-calculated using the control TMD value. Mix designs were then developed, separately, for each batch of control and PCM based on a target density of 96% of the TMD. Samples were produced and subjected to bulk specific gravity (BSG) testing and thermal testing in the GLC to determine the volumetric and thermal properties of each mix for comparison with the specification.

3.5.1 Aggregate Gradation Analysis

The ASTM C-136 standard was followed to obtain the gradation of the individual aggregate stockpiles used for batching the HMA cubes. For the mix design, a specific gravity of 2.70 and absorption of 1.1% were averages of known properties used for the NWA.²⁰ Once the gradations were obtained for each stockpile, a linear combination of stockpiles was used to obtain a full aggregate gradation that was within the limits given in the Superpave specification.

3.5.2 Theoretical Maximum Density Test, Sample Mix Design, and Production

Once the aggregate gradation was determined, a trial binder content of 5.5% was selected and a mix was batched for the TMD test. This binder content was selected as an initial point to attempt to find the optimal content to yield the desired mix volumetric properties. In order to obtain the TMD of the mix, a loose sample was required. The mixing procedure was altered so that instead of pouring the mix into molds, it was cooled to room temperature during a period of continuous mixing. Once the sample had fully cooled, the TMD test could begin, following the CoreLok procedure explained in Appendix D. After experimentally determining the TMD of a control batch, the expected TMD of a PCM batch was back-calculated using these results.

With the known TMD values for each batch, a mix design was prepared to produce samples with a target air void content of 4%. Once each mix design was completed, a control

batch and a batch of 1.25% PCM-6 were made according to the mixing procedure in Appendix E. Tables 10 and 11 contain the final mix designs developed and implemented for the Phase 3 samples.

Table 10: Mix design for control batch.

Mix Component	Mass (g)
NWA	840
Coarse Aggregate	141
Crushed Stone	360
Natural Sand	339
Binder	48

Table 11: Mix design for 1.25% PCM-6 batch.

Mix Component	Mass (g)
NWA	720
Coarse Aggregate	141
Crushed Stone	360
Natural Sand	219
LWA	81
No. 4	81
PCM-6	11
Binder	45

3.5.3 Bulk Specific Gravity Test and Volumetric Calculations

Once the cubes cooled overnight, the BSG test was conducted on each sample according to ASTM D7063 and the CoreLok procedure explained in Appendix F. The BSG values for these samples were used along with the recorded masses of aggregate and binder in each cube to calculate volumetric properties, including the percent voids in total mix (VTM), the percent voids in the mineral aggregate (VMA), and the percent voids filled with asphalt (VFA). These data were compared against each sample and the specifications to determine the effect of the PCM on volumetric properties, as well as adherence to the Superpave specification.

3.5.4 GLC Testing in Phase 3

Phase 3 utilized three control samples and three samples of 1.25% of PCM-6. Due to time constraints, only one control and two samples of 1.25% PCM-6 were tested. These tests followed the same logic as Phase 2. The main differences were that the Phase 3 testing utilized a more gradual temperature change of 2 °C/hr for cooling and 4 °C/hr for heating, and contained only one cycle that ranged from 25 to -25 °C (Figure 13).

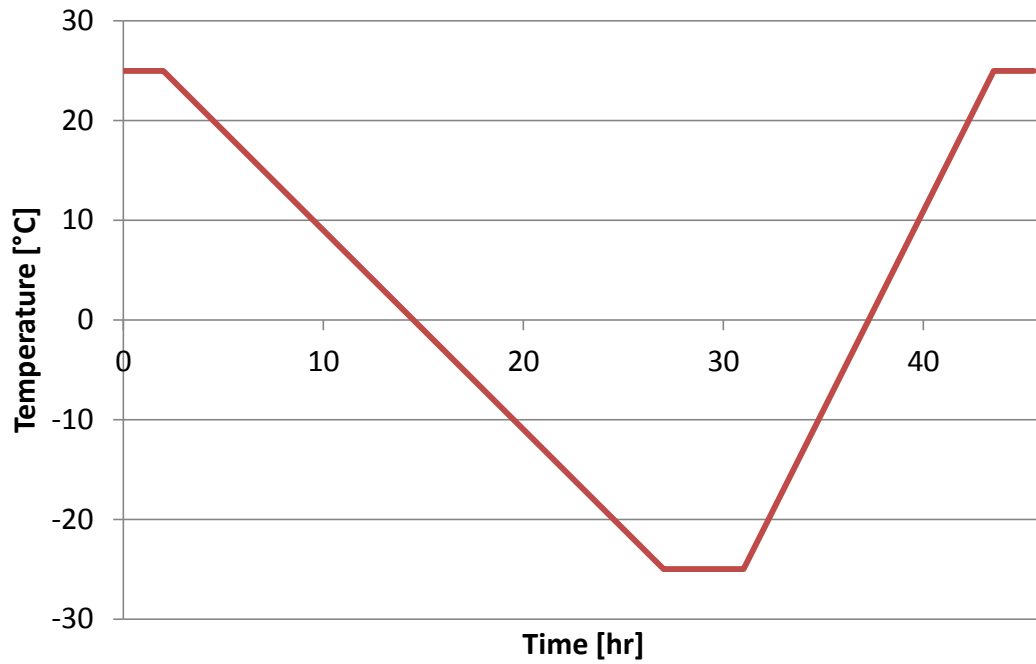


Figure 13: GLC cycle for Phase 3 thermal property testing.

The more gradual temperature change was used because it was expected to produce more consistent temperature measurements near the phase change temperature and allow for more accurate computations of thermal conductivity (Equations 6 and 7).²¹

4 Results and Discussion

4.1 Phase 1: Heating and Evaporation Tests

The feasibility of incorporating PCM-6 into HMA was investigated to ensure the PCM-6 would not combust at the high temperature (150 °C) used in asphalt production. A sample of PCM-6 was placed in the oven and checked periodically for combustion. During the one hour test, no combustion was observed. The sample of PCM-6 was weighed before and after heating, and a weight change of 6.86% was calculated.

Because the PCM-6 would be incorporated into the asphalt samples via absorption into LWA, absorption tests were used to determine the absorption levels for each LWA sieve size. Six samples of each sieve size were tested (Table 12). No. 8 sieve produced results similar to the theoretical value of 13.3%, which was the calculated value for absorption of PCM-6 into LWA. In general, the finer LWA material absorbed more PCM-6 than the coarser LWA, but this increase may be the result of PCM-6 adhering to the surface of the LWA due to the larger surface area per volume.

Table 12: Absorption test data.

Sieve Size	LWA/PCM Percentage (%)	Standard Deviation
No. 4	10.1	0.509
No. 8	13.3	0.532
No. 16	18.1	0.632
Blend	11.9	0.279

After completing the absorption test, evaporation tests were conducted to determine the rate of evaporation of PCM-6 at 150 °C. For these evaporation tests, the LWA saturated with PCM-6 was placed in an oven at 150 °C and weighed every 30 minutes. Upon completion of the test and analysis of the results, it was found that for each sample over 70% of the PCM-6 had evaporated within the first 30 minutes (Figure 14). When the samples were removed from the oven after the first interval, it was noted that the surfaces were no longer glossy. The lack of gloss indicated that some portion of the PCM had adhered to the surface and evaporated. Because of the quick rate of evaporation, a second test with a shorter time interval was conducted to obtain more detailed information on the evaporation of PCM-6 from LWA.

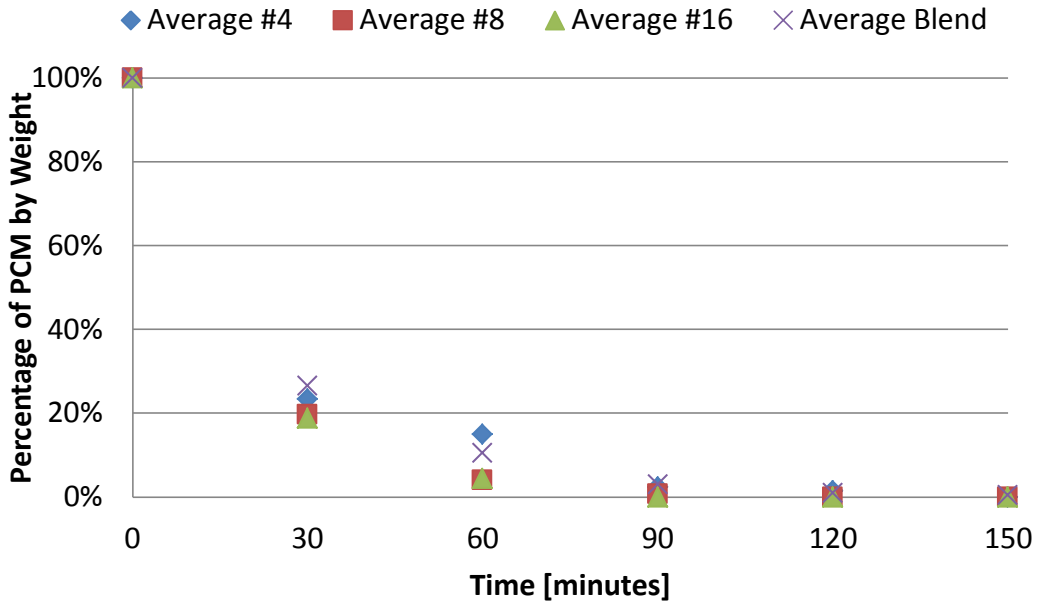


Figure 14: First PCM-6 evaporation test.

Because the majority of the PCM-6 evaporated from the LWA within the first 30 minutes, each new sample was measured at 5-minute intervals. With the data from this second evaporation test, it was found that after 5 minutes approximately 15% of the PCM-6 would evaporate (Figure 15).

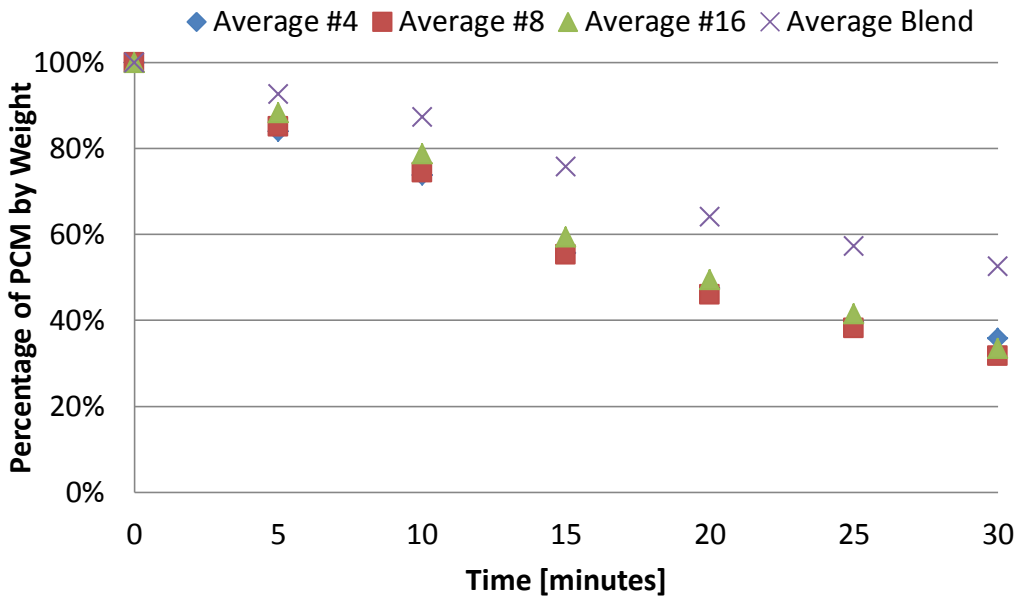


Figure 15: Second PCM-6 evaporation test.

These series of tests established that PCM-6 would not combust at 150 °C and that high-temperature exposure will quickly evaporate the PCM-6. Because of high evaporation rates, the

mix design was altered to minimize the exposure of the LWA/PCM-6 mixture to high temperatures.

4.2 Phase 2: Sample Production and Thermal Testing

4.2.1 Sample Production and Mix Designs

The first samples produced were control cubes containing no PCM-6. During the mixing process, it was determined that the content of fines was too large for the 5.5% binder content, and extra binder was added to give a final content of 10.4% for the control batch. The cubes were compacted and extracted from the molds successfully; however, only two samples could be produced from the size of the batch of HMA that was mixed.

After producing the control cubes, the mix design was altered to use a binder content of 9%. Construction of the 1.25% PCM-6 batch was successful, although the top surface was slightly rougher due to an inadequate amount of soap solution used on the tamp during compaction (Figure 16).



Figure 16: Compacted HMA samples with 1.25% PCM-6.

During production of the 10.5% PCM-6 batch, more frequent soap spray was applied to the tamp in order to provide a smoother surface. However, production of the 10.5% PCM-6 samples was unsuccessful. The mix was designed to simulate a pavement with the maximum amount of PCM-6 incorporated as possible. During the mixing process, it was noted that the HMA had a visible sheen to it, different from previous batches. Additionally, it was noted that the mix was more difficult to compact, which may have been due to the gradation consisting of only material from the No. 4 to the No. 16 sieves. During extraction, an oily residue was observed at the bottom of the molds, and when the forms were removed the samples fell apart (Figure 17). The degradation of the structural integrity was hypothesized to have been caused by

excessive PCM-6, such as from material on the surface of the aggregate particles, interfering with the ability of the binder to coat and bond with the aggregate particles. Due to the inability to form samples, this batch could not be tested in the GLC.



Figure 17: Samples with 10.5% PCM-6 after demolding.

To improve the maximum amount of PCM incorporated into a batch, first the mix design was altered to consist of roughly 50% LWA by weight, which corresponds to 5.5% PCM. Second, normal weight aggregate was used to aid in adhesion of the mix particles, as well as provide more fines content to fill in the voids between coarser particles. Also, when preparing the LWA soaked in PCM-6, the mixture was allowed to air dry for 4 hours after the 24 hour soaking period in order to reduce the amount of PCM-6 on the surface of the LWA. This batch still had a visible sheen to it during mixing. After demolding the samples, they fell apart immediately, just as the 10.5% PCM batch did. This resulted in no viable samples for thermal testing and the conclusion that 50% LWA/ 5.5% PCM-6 was still too high to make a feasible mix.

After, a mix was designed to incorporate 2.5% PCM-6. In an attempt to minimize the PCM-binder interaction on the surface of the aggregates, the LWA gradation was changed to eliminate the No. 16 sieve size which retained too much PCM on the particle surface. These samples compacted better and were successfully extracted from the molds. The samples were left to cool overnight to ensure adequate strength before removal from the mold plate. After removing the samples, several observations were made. First, these samples were much weaker than the 1.25% PCM-6 samples and required extra care during handling to ensure samples did not crack or fall apart. A theory for the weaker samples was that due to the large proportion of course materials contributed by the LWA, the samples did not compact as well by hand as a

normal gradation might. A second observation was that during sample handling the bottom surface of each cube was stickier to the touch than any other surface. It is theorized that this might be due to PCM migration to the bottom of the sample by gravity through the air voids. Upon further examination of the samples, a color difference among the aggregates was also noted (Figure 18). A theory for this difference in shading is that the lighter shaded aggregates are LWA which have not been adequately coated with binder due to PCM-binder interactions which could affect the strength of the samples.



Figure 18: Observed difference in color shading on faces of cubes with 2.5% PCM-6.

At the end of the Phase 2 mix design and production process, it was found that the maximum feasible PCM content that can be incorporated in an HMA sample using LWA absorption was approximately 2.5%.

4.2.2 GLC Testing in Phase 2

In total, 9 samples with 27 trials (9 cooling/heating cycles) were conducted using the Guarded Longitudinal Calorimeter (GLC) during Phase 2 of testing. Temperature profiles for all trials are found in Appendix H. In order to determine the thermal impacts of incorporating PCM into HMA, two types of graphs were analyzed: average temperature of the sample versus the heat flow across the sample, and the average temperature of the sample as a function of time. The average temperature of the sample was the average of the temperatures measured by thermocouples T_1 and T_2 .

The purpose of measuring the average temperature versus heat flow of the sample was to determine if there was an increase or decrease in the heat flow through the sample at the phase change temperature of 6 °C. When the sample was subjected to freezing, an exothermic reaction

was expected and, conversely, when the sample was subjected to thawing, an endothermic reaction was expected. The reactions, if large enough, would appear as spikes in the heat flow. Each sample was subjected to one trial that included three cooling/heating cycles (Figure 19).

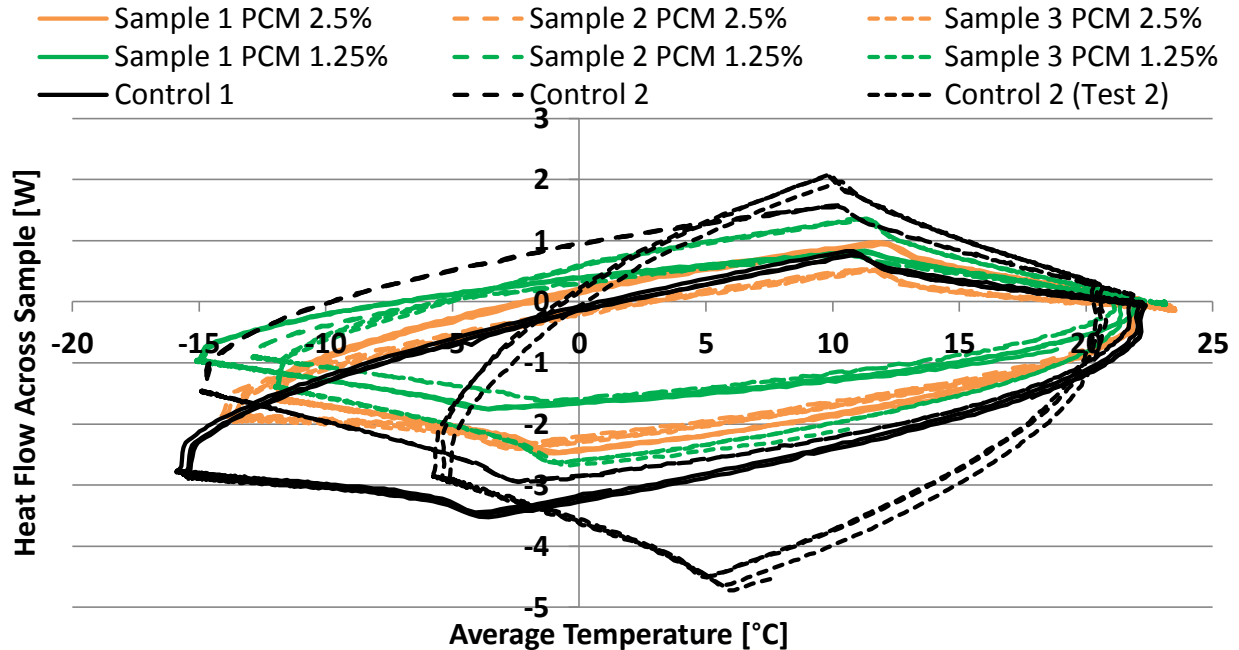


Figure 19: Phase 2 heat flow versus average temperature for samples.

The results from the GLC were mixed, with 2.5% and 1.25% PCM-6 samples producing relatively centralized data, while the controls produced less consistent results. All samples underwent the same cooling/heating temperature profile and were conducted in approximately the same ambient temperature. Although spikes were seen in the data (quadrants 1 and 3 of Figure 19), the spikes were present for all samples and likely caused by the transition from the constant rate of decreasing/increasing temperature to a constant temperature. Because of the lack of notable spikes, Figure 19 shows no conclusive evidence that endothermic or exothermic reactions occurred during phase change of the PCM-6.

Another method for analyzing the Phase 2 GLC data was to analyze the average temperature versus time (Figure 20). This method measured the time taken for a sample or control to freeze/thaw and the extreme hot and cold temperature values. Even though the PCM did not produce notable energy changes (Figure 19), the impacts of the PCM may be evident in the reduction of extreme temperatures and decrease of the rate of cooling/heating. Because the cooling/heating cycles all started at 23 °C, it was possible to normalize all data to the instant the temperature started decreasing by monitoring when the thermocouple nearest to the cold plate

(T_o) began decreasing. The normalization of the data refers to the separation of the three cooling/heating trials into separate graphs. Each of the graphs start with the maximum temperature measured before the sample began cooling. For the second and third cycles, the sample never reached exactly 23 °C, so the maximum measured temperature was utilized for normalization. After normalizing all trials, the individual cycles were averaged to create data for overall averages for each sample and control (Figure 20).

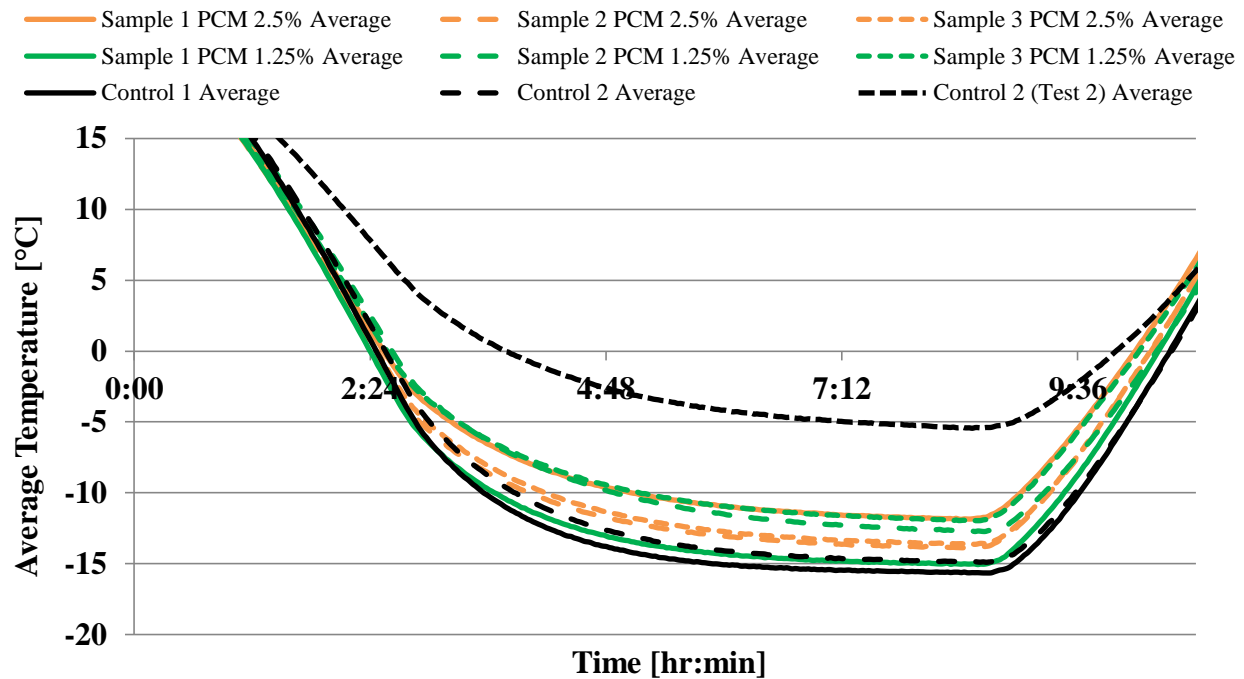


Figure 20: Average temperature versus time for sample averages.

For both the samples and controls, the largest temperature deviations occurred after freezing. The thermocouple nearest to the sample (T_o) indicated all samples were subjected to the same programmed cooling/heating cycles in, roughly, the same ambient temperature. Although Control 2 and Control 2 (Test 2) were the same sample, Control 2 (Test 2) produced different results. The most probable explanation for the difference was improper use of the GLC, which could include poor contact between the thermocouples and the sample, which would lead to improper temperature readings, and/or an inadequate seal between the GLC and the top cover, which would allow ambient air to circulate inside the device. For the following Phase 2 analyses, Control 2 (Test 2) was treated as an outlier.

Because Figure 20 was comprised of the average of three normalized cycles, an analysis was conducted to assess the individual trials to understand the uncertainty with the data. Trials for PCM 2.5% were used as an example and provide information on individual trials (Figure 21).

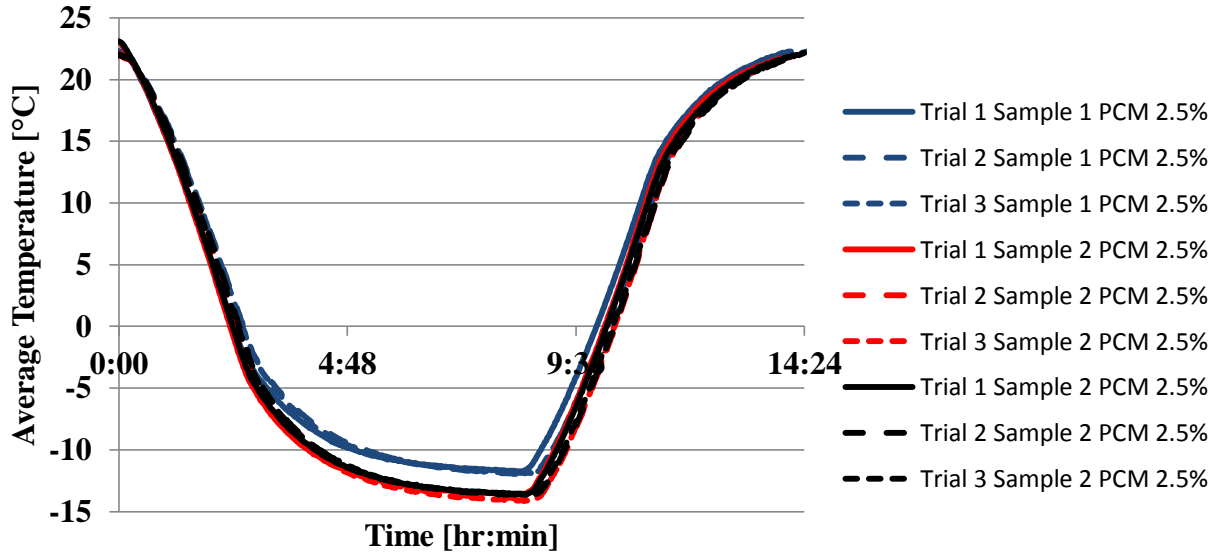


Figure 21: Data from all cycles of PCM 2.5%.

Although the samples with the same concentration of PCM produced slightly different temperature profiles, most trials were grouped closely. For all trials, the average standard deviation never exceeded 0.5 °C. A summary of the average and maximum standard deviations demonstrates the small deviations between samples (Table 13).

Table 13: Maximum and average standard deviations for sample cycles (1 cycle = 3 trials).

Sample	PCM 2.5%			PCM 1.5%			Control		
	1	2	3	1	2	3	1	2	3
Maximum [°C]	1.28	1.17	0.87	0.50	0.36	0.88	0.43	0.76	1.15
Average [°C]	0.46	0.42	0.30	0.13	0.21	0.29	0.18	0.34	0.49

After assessing the trial averages, overall sample averages and standard deviations were computed for the control, 1.25% PCM and 2.5% PCM samples to determine the average extreme temperature and average freezing time (Figure 22). The dotted lines represent one standard deviation (σ) and Control 2 (Test 2) was not included in the computations.

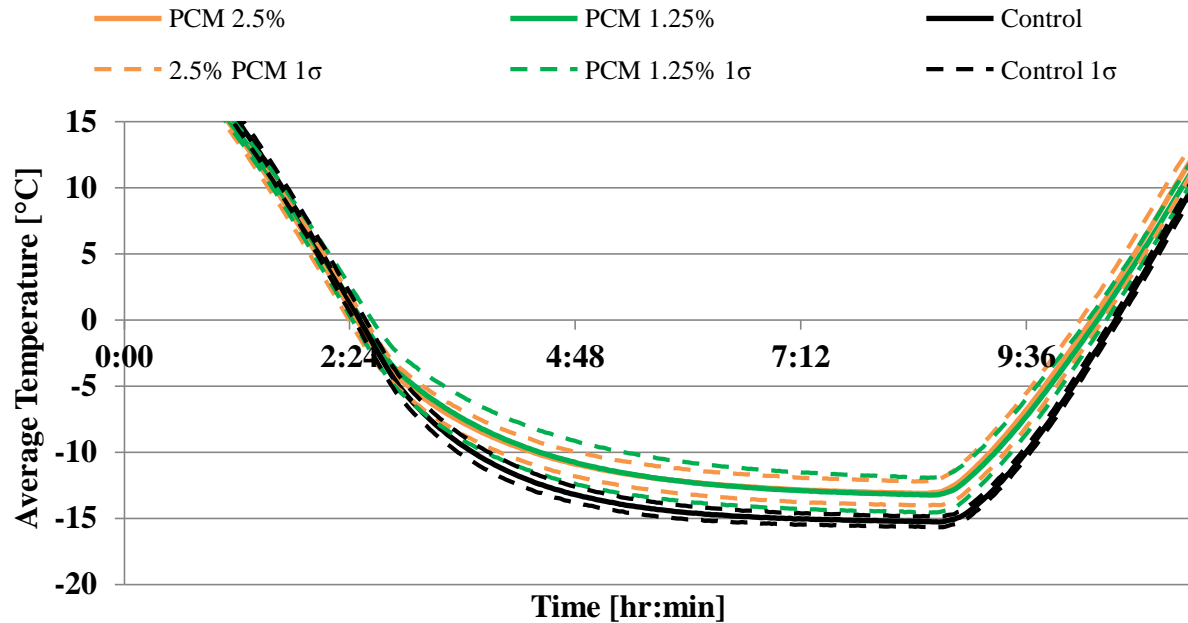


Figure 22: Phase 2 trial average temperature versus time.

The approximate time for a sample or control to freeze was estimated by the time it took for the average temperature to reach 0 °C. Figure 22 indicates the average samples and controls froze after approximately 2.3 hours into a cycle. Although no PCM sample prevented freezing, a noticeable change in the cooling rate was observed at approximately 30 minutes after the phase change temperature. This reduction in the cooling rate, on average, reduced the average temperature of the PCM samples when compared with control. The lowest average temperatures for 2.5% PCM, 1.25% PCM and control were, respectively, -13.11 °C, -13.24 °C and -15.28 °C. Although there is a large deviation of temperature with the control average, the data from 1.25% PCM and 2.5% PCM, even with one standard deviation, indicates PCM may reduce extreme cold temperatures when compared with the control.

Although the PCM was chosen specifically to prevent or reduce freezing, the extreme hot temperatures of the samples were analyzed (Figure 23). Figure 23 is the same as Figure 22, except the range of data has been modified. Because the first trial was allowed to reach 23 °C without regard to time, only the second and third trials were used in order to keep a consistent time interval. Doing so, the average extreme hot temperatures for 2.5% PCM-6, 1.25% PCM and control were 22.08 °C, 21.62 °C and 21.59 °C, respectively.

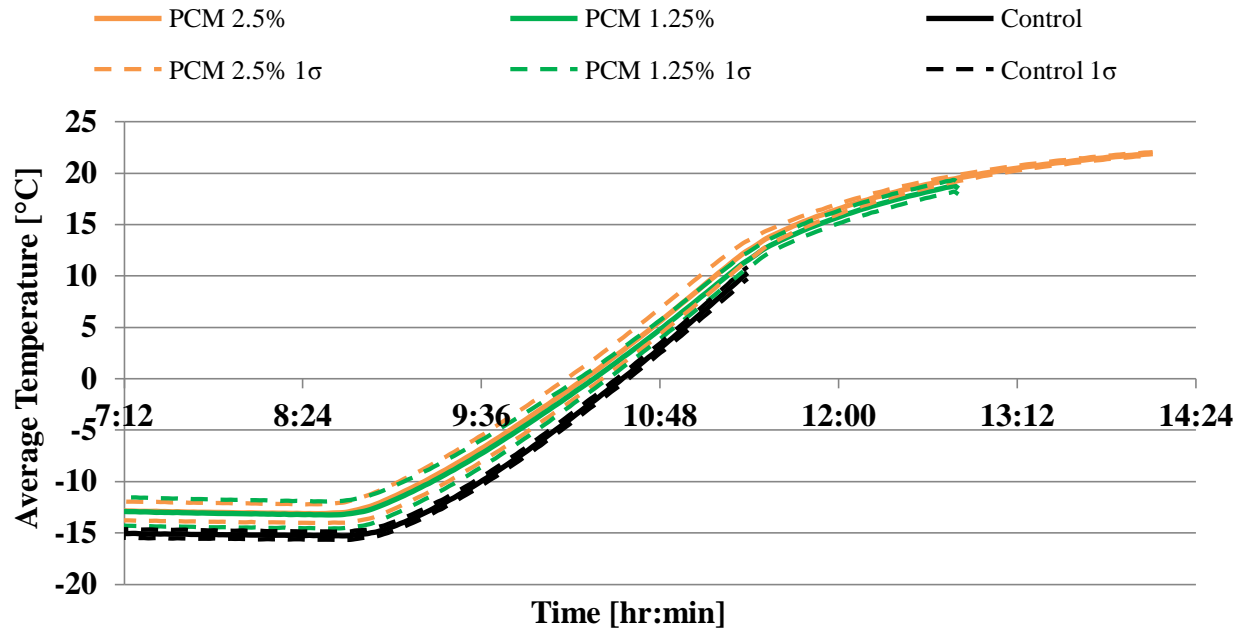


Figure 23: Trial averages at approximate phase change temperature (thawing).

Another potential benefit of the PCM was that samples may thaw quicker than the controls due to the lower extreme temperature achieved by the sample (Figure 23). The difference between the PCM samples and control was approximately 12 minutes. Ideally, Figure 23 would contain an equal number of data points for each sample. One reason for the difference in the amount of data points was due to the multiple cooling/heating cycles being separated into individual trials. If the samples did not reach steady-state, theoretically, the maximum temperature would occur just before the GLC began cooling. In practice, due to small fluctuations in the temperature, the maximum temperature sometimes occurred prematurely. The maximum temperature was used as a marker to indicate a new cycle had begun, and if premature, would cause some cycles to have slightly more or less data points. For the control sample average, the reduction was because Control 2 had prematurely stopped recording during the final heating cycle. Although many samples ran the proper length of time, sample averages and standard deviations were limited by the amount of data points of the smallest sample. For a more accurate representation of the ability of PCM to reduce extreme temperatures, Appendix H should be used. Appendix H provides evidence that for some samples of PCM-6 the extreme hot temperature was reduced, the rate of heating was reduced, and the samples thawed quicker than controls.

One limitation with measuring the PCM was that each PCM sample was only estimated to contain the designed content, but no tests were conducted to determine how much PCM remained in the sample after mixing. Future tests could be improved if a more accurate PCM content could be measured after mix production. In addition, since there was no consistent mix design, some of the observed thermal differences could be attributed to different binder content and/or different types and sizes of aggregate. Future tests should be conducted to determine if the thermal properties of aggregate varies greatly in order to reduce uncertainties in the data. Because of the greatly differing results between Control 2 and Control 2 (Test 2), future studies should investigate the consistency and quality of the data produced by the GLC. One method for assessing the GLC would be to subject both controls and samples to multiple cycles on the GLC and assess potential differences. To improve upon Phase 2 testing, during Phase 3 methods for improving sample construction and data measuring were investigated. The changes include reducing the rate of change for the GLC cooling/heating cycle in an attempt to more accurately observe the effects of PCM, and mixing the samples using a consistent mix design to reduce thermal uncertainties.

In conclusion, Phase 2 results provided within one sigma that thermal improvements could be obtained with the incorporation of PCM-6 into HMA. The results show that PCM-6 may reduce the extreme cold temperature of a sample, the rate of cooling, and decrease the time for the sample to thaw. There was no conclusive evidence to support that utilizing PCM-6 reduces the extreme hot temperature. However, in order to have more certainty with the data, future testing would have to be conducted to investigate methods for determining exact PCM content and for producing more consistent GLC data.

4.3 Phase 3: Improved Mix Design with Volumetric and Thermal Testing

4.3.1 Aggregate Gradation Analysis

Three stockpiles were used to generate an acceptable gradation: 3/8 in coarse aggregate, crushed stone, and natural sand. Two gradations were developed which fell between the Superpave specification limits (Figure 24). The first was a linear combination of the three stockpiles which consisted of 40% material from the 3/8 in coarse aggregate stock, 20% material from the crushed stone stock, and 40% material from the natural sand stock. The second gradation consisted of the linear combination with some alterations. During the mixing process in Phase 2, it was observed that aggregate particles retained on the 3/8 in sieve or higher

interfered with compaction of the 2 in cube samples. This interference was due to the small size of the samples and the corners present in the compaction mold. In order to improve compaction, material retained on or above the 3/8 in sieve was removed from the aggregate gradation and replaced with an equivalent percentage of material retained on the No. 4 sieve.

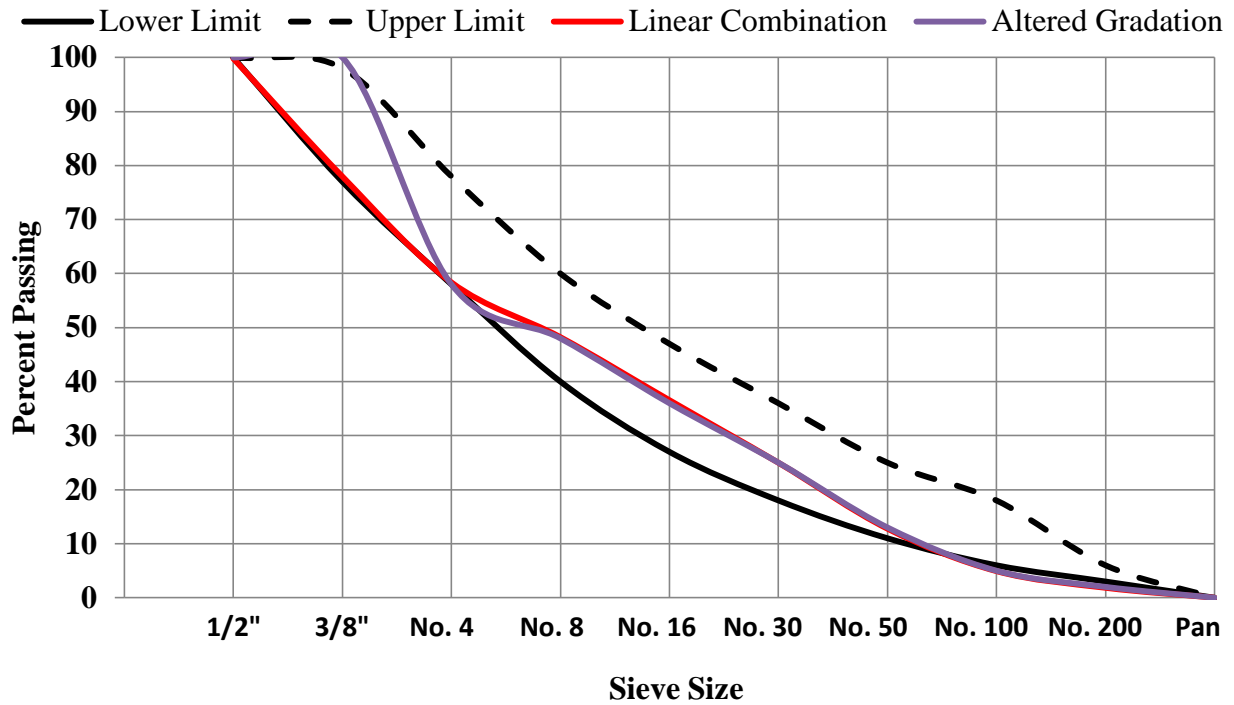


Figure 24: Plot of aggregate gradations for HMA mixes.

It should be noted that this altered gradation was not able to satisfy the Superpave specification due to the high natural sand content. A typical mix would incorporate a maximum of 20% natural sand; however, due to the uniformly-graded nature of the 3/8 in coarse aggregate stock, more natural sand and crushed stone stock was needed in order to provide a gradation within the limits of the specification. If this gradation were to be used in practice, it would be more expensive and may impact the properties of the HMA mix. Therefore, the stockpile proportions and alterations used for this gradation were only made in order to facilitate lab operations using the materials available and the non-standard cube samples needed for the GLC tests.

4.3.2 Theoretical Maximum Density Test, Sample Mix Design, and Production

After performing the theoretical maximum density test (TMD) twice on each of three loose material control samples, the average TMD value was reported as 2.34 g/cm³ with a standard deviation of 0.11 g/cm³. A table with all raw data for these calculations is located in Appendix I. The back-calculated TMD for the PCM samples was 2.29 g/cm³.

The first batch of samples produced was the control batch. In order to produce samples with the desired volumetric properties, it was essential to combine all of the material into the mold without losses. As the temperature of the mix dropped below optimal during the compaction process, it became more difficult to combine the material. Minor material losses were observed for each sample; however, all samples did compact and extract easily, and were in acceptable shape for volumetric testing.

The final batch of samples produced was the 1.25% PCM-6 batch (Figure 25). Minor material losses were observed in these samples during compaction. The temperature had dropped significantly below the optimal compaction temperature before the final sample was made, so the mold with 2 compacted samples was placed back in the oven for 5 minutes. Although not measured, small losses of PCM-6 were expected. All samples were extracted in good condition and were allowed to cool before volumetric testing.



Figure 25: Phase 3 batch of 1.25% PCM-6 samples after demolding.

4.3.3 Bulk Specific Gravity Test and Volumetric Calculations

Average values for the three volumetric properties in question (VTM, VMA, and VFA) were calculated using information from the mixing process and the bulk specific gravity test (Table 14). All raw data for these calculations can be found in Appendix J. The bulk specific gravities were 84% of the TMD, slightly lower than desired, which was expected due to the

material lost during compaction of each sample. The BSG results, however, also impacted the other volumetric properties which were skewed. The voids in the total mix (VTM) were the most notable as they were off by a factor of four.

Table 14: Volumetric properties of HMA samples.

Property	G _{mb}		VTM (%)		VMA (%)		VFA (%)	
	Average	St Dev	Average	St Dev	Average	St Dev	Average	St Dev
Target	Control 2.25 / PCM-6 2.20		4		15		65-78	
Control	1.97	0.11	16.0	4.8	31.1	4.1	49.3	8.3
PCM-6	1.92	0.01	16.2	0.5	32.7	0.4	50.5	1.0

Although the properties were not in line with the specification, some observations were informative. The average properties for the controls and the PCM samples were approximately the same, suggesting that the PCM may not have a large effect on the volumetric properties of the HMA. In addition, the standard deviation among PCM samples was low, indicating that there was high precision in these results. The relatively higher standard deviation among the controls could be due to the first sample tested. During the BSG test, this sample showed signs of leakage in the vacuum-sealed bag, and had to be dried overnight before retesting.

4.3.4 GLC Testing in Phase 3

Phase 3 thermal testing utilized an improved mix design and slower GLC cooling/heating cycle. Because of time constraints, one control and two samples of PCM-6 1.25% were tested. Each sample was subjected to one cooling/heating cycle in the GLC. In total, three samples of PCM 1.25% and Control were mixed. Control 2 was selected as the test sample because, visually, it was the most structurally sound sample.

The heat flow across the sample was plotted as a function of the average temperature (Figure 26). As was the case for Phase 2, the purpose was to determine if there was any change in heat flow near the phase change temperature. In comparison to Figure 19, Figure 26 was comprised of only one cooling/heating cycle for each sample.

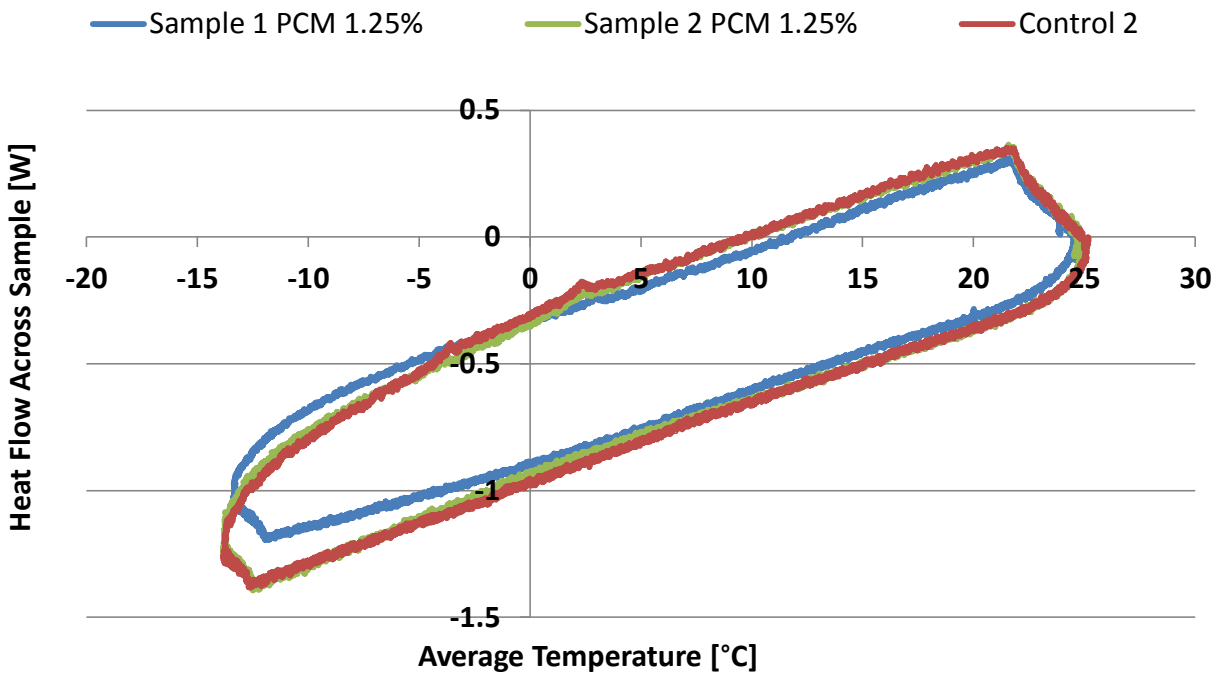


Figure 26: Phase 3 heat flow versus average temperature for samples.

Figure 26 shows no signs of endothermic or exothermic reactions at the phase change temperature. Although a small spike was observed at 2.5 °C for Control 2, no spike was observed for any of the PCM samples. In addition, Sample 2 PCM 1.25% and Control 2 produce a similar curve, while Sample 1 PCM 1.25% produced a smaller shape.

After, the average temperature was then plotted as a function of time. The graph allows for analysis of the rate of cooling/heating, freezing/thawing times, and the computation of maximum temperatures (Figure 27).

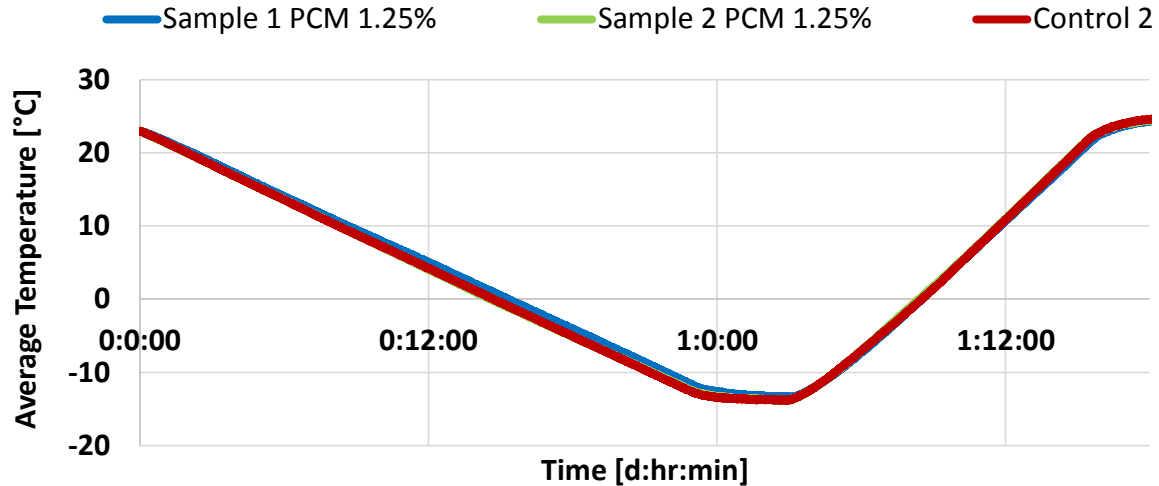


Figure 27: Phase 3 trial average temperature versus time.

As was the case in Figure 26, Sample 2 and Control 2 produced almost identical temperature profiles, while Sample 1 showed a decrease in the freezing rate. A summary of the cooling/heating rate, extreme temperatures and thermal conductivity are shown (Table 15):

Table 15: Phase 3 extreme temperatures, freezing/thawing times and thermal conductivity.

	Sample 1 PCM 1.25%	Sample 2 PCM 1.25%	Control 2
Maximum Temperature [°C]	24.8	24.8	24.9
Minimum Temperature [°C]	-13.4	-13.8	-13.8
Thermal Conductivity [W/mK]	0.65 (+/- 0.07)	0.83 (+/- 0.11)	0.83 (+/- 0.11)
Freezing Time [d:hr:min]	0:15:17:10	0:14:35:10	0:14:41:40
Thawing Time [d:hr:min]	1:8:31:30	1:8:24:40	1:8:31:40

All samples had approximately the same extreme temperatures and thawing time, but the rate of cooling was reduced for Sample 1. It was expected that all samples would reach the approximate same maximum and minimum temperatures because of the length of the test. Sample 1 remained above freezing for approximately 35 minutes longer than Control 2. It is important to note that during Phase 3 testing, the GLC changed temperature every hour, whilst during Phase 2 the GLC changed temperature every minute. In addition, the duration and cycling between cooling/heating also causes Phase 2 results to appear more substantial than Phase 3.

Another method for analyzing the thermal characteristics of the samples was to compute the thermal conductivity using Equations 6 and 7, which was provided by ASTM E1225-9. Sample 1 had an average thermal conductivity of 0.65 W/mK, which was lower than Control 2

and Sample 2. A lower conductivity reduces the rate of heat flow through a sample which reduces the rate of cooling and heating. Although the reduction in heating rate could potentially increase the time it takes for a sample to thaw, the sample could still thaw quicker (Sample 1) or on par with a control (Sample 2) if the PCM reduced the extreme cold temperature. Because Control 2 and Sample 2 exhibited roughly the same results, future analysis should be conducted to determine if any PCM was integrated into Sample 2 or if the GLC recorded inaccurate results. Although more tests will need to be conducted to be certain of the effects of PCM, these initial results provide additional indications that HMA incorporated with PCM reduces cooling rates and, potentially, extreme cold temperatures.

One issue with utilizing a slower cooling/heating temperature profile was that the temperature inside the sample varied. This variance meant PCM located closer to the cold plate would have changed phase sooner than PCM located near the top of the sample. This difference in activation time would diminish the collective ability of the PCM to warm or cool the sample. For example, the temperature profile of Sample 1 PCM 1.25% (Phase 3) is shown (Figure 28).

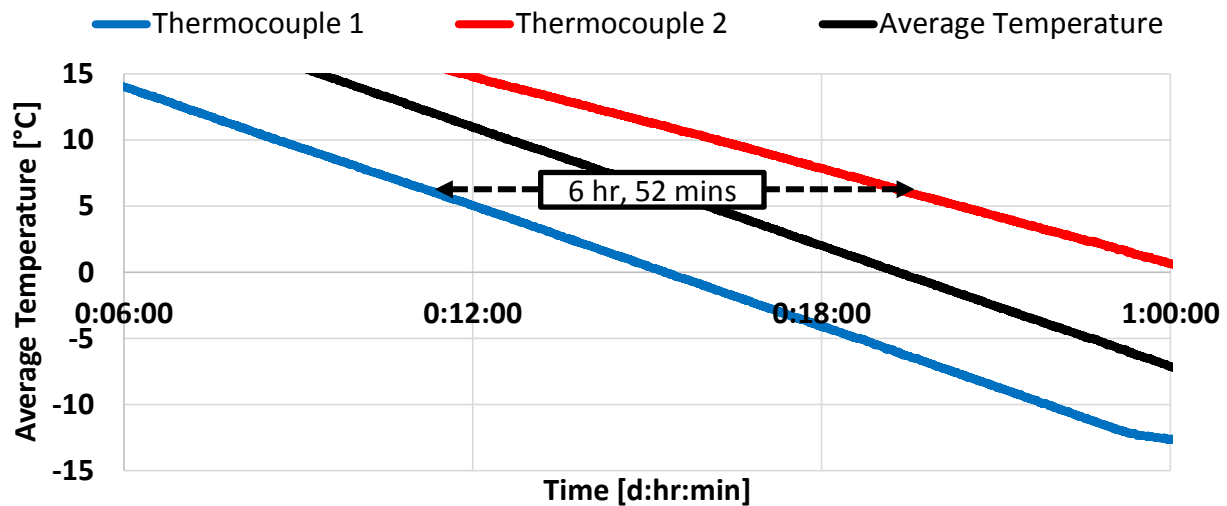


Figure 28: Temperature profile of sample 1 PCM 1.25% (Phase 3).

The figure illustrates that by the time thermocouple 2 (T_2) indicated 6 °C, thermocouple 1 (T_1) had reached 6 °C almost 7 hours earlier. In addition, by the time all of the PCM, theoretically, had changed, portions of the sample would have already frozen. For comparison, the temperature profile of Sample 1 PCM 1.25% (Phase 2) is shown (Figure 29).

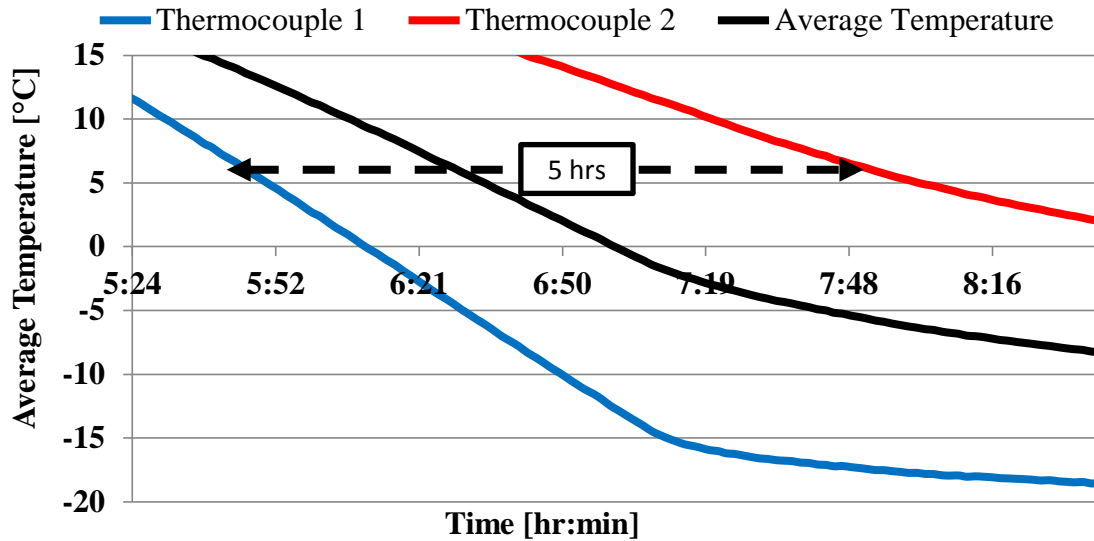


Figure 29: Temperature profile of sample 1 PCM 1.25% (Phase 2).

In comparison with Phase 3, the Phase 2 sample, theoretically, completed its phase change in approximately 5 hours. Although the amount of PCM and particle size distribution was different between the two test phases, a portion of the different temperature profiles was caused by the rate of PCM activation. In the future, endothermic and exothermic reactions may be more observable if the temperature decreased/increased more quickly so that the PCM would change phase in a shorter amount of time, thus releasing more energy at once.

Even though Phase 3 attempted to improve upon the results of Phase 2 by removing uncertainties in the data, there are still improvements that can be made for future work. Although a slower cooling/heating temperature profile was expected to facilitate measuring the phase change, in reality, the slower cycle most likely caused the PCM to activate so slowly that the change was not easily observable. For future tests, different cooling/heating cycles and types of PCM should be tested to better understand how the PCM responds to different extreme temperatures and temperature cycling. For instance, one experiment might test a PCM sample with a gradual cooling rate that reaches an extreme cold temperature, while another might explore a quick cooling rate that reaches a less-extreme cold temperature. Having a better understanding of the response of the PCM will be useful in deciding which PCM is suited for given conditions. Although Phase 3 utilized a consistent mix design, the thermal properties between the PCM-6 samples and control samples were not completely the same since volumetric changes between the LWA and NWA may have caused changes in the thermal conductivity of

the block. Because LWA was selected as the method for incorporation, it was not possible to create complete consistency between the controls and samples. Instead, the thermal properties of LWA and NWA would have to be assessed to determine if there are any significant differences. In addition, methods for measuring the PCM content in the sample should be investigated.

5 Conclusions and Future Work

The incorporation of PCM-6 into HMA using LWA was shown to be possible, but was not yet feasible for use in airports. The data provided evidence that the incorporation of PCM altered the thermal properties of the sample, but at the cost of a reduction in the strength of the sample. Although no strength tests were conducted on the samples, many of them were easily damaged during testing and handling. Further research should be conducted to determine the effects of LWA on the mechanical properties of the HMA and to determine the interaction between the PCM and the binder. Other methods of introducing PCMs into HMA that isolate the PCM from the binder should be investigated. Encapsulating the PCM in a pellet may be a viable option, for instance, because it isolates the PCM from the binder while still dispersing it throughout the matrix of the HMA. In addition, the volumetric property testing completed in Phase 3 indicated that PCM-6 does not have an adverse effect on volumetric properties, such as air voids, when compared to a control sample. However, this should be verified using the proper Superpave mix production procedure instead of the hand compaction methods used in this study. Testing for both the volumetric and thermal properties of individual samples may be facilitated if the GLC was altered to work with cylindrical samples.

Overall, both Phase 2 and Phase 3 testing provided indications that it was possible to incorporate PCM-6 into HMA using LWA. The data showed that PCM reduced the extreme low temperature of a sample, reduced the rate of cooling, and decreased the time for the sample to thaw. Initially, PCM-6 was selected because it had a phase change temperature above the freezing point of water, but experimentally it did not prevent freezing from occurring. In addition, it was observed that samples behaved differently when subjected to slower or quicker cooling/heating cycles. For future tests, different cooling/heating cycles and types of PCM should be tested to better understand how the PCM responds to different extreme temperatures and temperature cycling. For instance, one experiment might test a PCM sample with a gradual cooling rate that reaches an extreme cold temperature, while another might explore a quick cooling rate that reaches a less-extreme cold temperature. Having a better understanding of the response of the PCM will be useful in deciding which PCM is best suited for given conditions. Potentially, composite samples comprised of multiple types of PCM could be designed in order to contend with different temperature fluctuations. Thus, there is a need for further research to make the incorporation of PCM into HMA practical.

References

- [1] Federal Aviation Administration. (n.d.). *Airports*. Retrieved from http://www.faa.gov/airports/planning_capacity/passenger_allcargo_stats/categories/.
- [2] Federal Aviation Administration, U.S. Department of Transportation. (2012). *Report to congress: National plan of integrated airport systems (NPIAS)*. Retrieved from http://www.faa.gov/airports/planning_capacity/npias/reports/media/2013/npias2013Narrative.pdf.
- [3] Federal Aviation Administration. (2012). *General aviation airports: A national asset*. Retrieved from http://www.faa.gov/airports/planning_capacity/ga_study/media/2012AssetReport.pdf.
- [4] Bargar, C., Langford, W., Prescott, J., & Stone, N. (2012, April 25). FODHippo an automated debris collection trend for airport runways.
- [5] Chen, W., Xu, Q., Ning, H., Wang, T., & Li, J. (2011). Foreign object debris surveillance network for runway security. *Emerald*, 83(4).
- [6] Bachtel, B. (1998). Foreign object debris and damage prevention. *Aero Magazine*, 1,1.
- [7] Aerosweep. Airfield FOD Sweeper - The FOD*BOSS. Retrieved from www.airport-technology.com.
- [8] Federal Aviation Administration. (2007). *AC 150/5380-6B, Guidelines and procedures for maintenance of airport pavements*. Second Edition. Washington, DC: USDOT.
- [9] Mallick, Rajib B. & Tahar El-Korchi. (2009). *Pavement engineering: Principles and practice*. Boca Raton, FL: CRC Press.
- [10] California Pavement Preservation Task Group. (2011). *Common distresses on flexible pavements*. Retrieved from Caltrans Division of Maintenance Web site: <http://www.dot.ca.gov/hq/maint/MTAG-CommonFlexiblePavementDistresses.pdf>
- [11] Hatton, E. (2006). *Washington airport pavement management system- Pavement management manual*. Champaign, IL: Applied Pavement Technology, Inc.
- [12] Transportation Research Board of National Academies. (2011). *ACRP Synthesis 22 - Common airport maintenance practices*. Washington, DC. Sponsored by the Federal Aviation Administration.
- [13] Dillingham, Gerald. (1998). *Airfield pavement: keeping nation's runways in good condition could require substantially higher spending*. Washington, DC: United States General Accounting Office. Report prepared for Senator John McCain.
- [14] Sakulich, A.R. & D.P. Bentz. (2012). *Incorporation of phase change materials in cementitious systems via fine lightweight aggregate*. *Construction and Building Materials*, 35 (2012) 483-490.
- [15] Joint Implementation Network. (n.d.). *Energy storage: Phase change materials for thermal energy storage*. Climate Tech Wiki: A Clean Technology Platform. Retrieved from <http://climatetechwiki.org/technology/jiqweb-pcm-0>.

- [16] Tannoury, G.A. (2007). *Laboratory evaluation of hot mix asphalt mixtures for Nevada's intersections- Phase II*. University of Nevada, Reno- Civil Engineering. ProQuest.
- [17] Lin, S. (2011). *Evaluation of HMA fracture mechanics-based thermal cracking model*. Unpublished Master's Thesis, Royal Institute of Technology, Stockholm, Sweden.
- [18] Sakulich, A.R. & D.P. Bentz. (2012). *Increasing the service life of bridge decks by incorporating phase-change materials to reduce freeze-thaw cycles*. *Journal of Materials in Civil Engineering*, 24 (2012) 1034-1042.
- [19] Cooley, A.L. Jr., et al. (2009). *Implementation of superpave mix design for airfield pavements*. Burns Cooley Dennis, Inc. Vols 1-3. Airfield Asphalt Pavement Technology Program.
- [20] El-Korchi, Tahar. Personal interview. 25 Nov. 2013.
- [21] Farnam, Y., Bentz, D., Sakulich, A., Flynn, D., and Weiss, J. Measuring Freeze and Thaw Damage in Mortars Containing Deicing Salt Using a Low Temperature Longitudinal Guarded Comparative Calorimeter and Acoustic Emission (AE-LGCC), Accepted for Publication in *Journal of Advances in Civil Engineering Materials (ASTM)*.

Appendices

Appendix A: Pure PCM-6 Heating Test

1. Weigh and fill a clean beaker with 20 mL of PCM-6.
2. Record the weight of the beaker with PCM-6 and calculate the mass of the PCM-6.
3. Place beaker in a ventilated oven at 150 °C for 1 hour.
4. At the end of the heating cycle, record the final weight of the beaker and calculate the amount of PCM-6 remaining.
5. Report the percent loss of pure PCM-6 per hour.

Appendix B: PCM-6 Absorption and Evaporation Tests

1. Record the mass of an empty mesh basket and fill it with a layer of LWA.
2. Record the filled weight of each basket before soaking.
3. After recording all weights, submerge baskets in the PCM-6 bath for 24 hours. Agitate baskets every 6 hours to allow air to escape from the samples.
4. After 24 hours, remove baskets from PCM-6 bath and allow drip-drying for 2 hours.
5. Reweigh the baskets and calculate amount of PCM-6 absorbed by LWA. Report percentages and compare with calculated theoretical absorption for PCM-6.
6. Place all baskets in the oven at 150 °C for 3 hours.
7. At half hour intervals record weights. Calculate percent loss of PCM-6.
8. Repeat measurements for 3 hours or until all the PCM-6 has evaporated.
9. Repeat steps 1-5 for 12 new samples.
10. Place all baskets in the oven at 150 °C for 30 minutes.
11. At five minute intervals record weights. Calculate percent loss of PCM-6.

Appendix C: Procedure for Mixing and Compacting Cube Samples with

Mechanical Mixer

A. Preparatory work

1. Place in oven at 150 °C, at least 3 hours before mixing:
 - Mixing bowl
 - Mixing blade
 - Aggregate on pans (LWA added to oven 2-5 minutes before mixing)
 - Molds
 - Binder
 - Sled
 - Spatulas (Putty knives)
 - Ladle
2. Gather other equipment for mixing and compacting process:
 - Gloves, lab coats, safety glasses
 - Soapy water spray (Dawn)
 - Tamp
 - Mallet
 - Scale
 - Temp gun
 - Sharpie marker
 - Viking mixer

B. Mixing

1. Place aggregate in mixing bowl
2. Place both on scale and zero
3. Add calculated binder amount (mass of aggr.)(%Binder)= x; x=mass of binder
4. Mix sample for 2 minutes
5. Wait for oven to return to 150 °C before mixing next sample (15 or so minutes)

C. Compacting

1. Place sled on scale and zero scale.
2. Put designated amount of mix into sled
3. Take out mold, spray with soapy water
4. Pour from sled into mold in one smooth motion
5. Use spatula to rod center 10 times
6. Rod each side 3 times
7. Spray bottom of tamp with soapy water
8. Place tamp on sample
9. Use mallet to hit tamp 16 times switching locations with each blow.
10. Use temperature gun to check sample temperature and allow to cool below 75 °C
11. Extract sample, allow to cool to room temperature, and label it.

Appendix D: CoreLok Procedure for the Theoretical Maximum Density Test

1. Ensure that CoreLok is set to Program 2
2. Place all three filler plates into CoreLok and remove sliding plate
3. Select a large bag and make sure that bag has no holes or stress points
4. Weigh the bag and one channel (corrugated, textured) bag and record total weight in column A
5. Weigh dry sample in air and record in column C
6. Place sample inside channel bag
7. With outer bag in the CoreLok, place channel bag textured side down inside outer bag
8. Use hand to gently spread mixture evenly over surface of textured bag
9. Push opening of channel bag away from opening of external bag. Channel bag must remain open for air flow out and channel bag should be about 1 in away from closed end of external bag
10. Place external bag opening over seal bar and close CoreLok (not channel bag opening)
11. After CoreLok runs, gently remove sample and transfer to water tub
12. While submerged, cut external bag open until 1 in is left connected. Do not cut channel bag.
13. Open both bags and allow water to enter for 15 seconds (if significant air bubbles out, dry sample and repeat sealing because bag was punctured)
14. Fold bags over and place on weighing basket while still submerged. Allow water to enter again and ensure bags do not touch sides or bottom of tank.
15. After scales stabilize, record weight in column D
16. Calculate the max specific gravity for the sample.

Appendix E: Procedure for Mixing and Compacting Cube Samples by Hand

Mixing

A. Preparatory work

1. Place in oven at 150 °C, at least 3 hours before mixing:
 - Mixing bowl
 - Aggregate on pans (LWA added to oven 2-5 minutes before mixing)
 - Molds
 - Binder
 - Sled
 - Spatulas (Putty knives)
 - Ladle
2. Gather other equipment for mixing and compacting process:
 - Gloves, lab coats, safety glasses
 - Soapy water spray (Dawn)
 - Tamp
 - Mallet
 - Scale
 - Temp gun
 - Sharpie marker

B. Mixing

1. Place aggregate in mixing bowl
2. Place both on scale and zero
3. Add calculated binder amount $(\text{mass of aggr.})(\% \text{ Binder}) = x$; $x = \text{mass of binder}$
4. Mix sample using the sled or spatula to scoop from the bottom of the bowl to the top. Repeat process, working around all sides of the bowl, ensuring all aggregate is coated in binder. Total mixing time should be 2-3 minutes.
5. Wait for oven to return to 150 °C before mixing next sample (15 or so minutes)

C. Compacting

1. Place sled on scale and zero scale.
2. Put designated amount of mix into sled
3. Take out mold, spray with soapy water
4. Pour from sled into mold in one smooth motion
5. Use spatula to rod center 10 times
6. Rod each side 3 times
7. Spray bottom of tamp with soapy water
8. Place tamp on sample
9. Use mallet to hit tamp 16 times switching locations with each blow.
10. Use temperature gun to check sample temperature and allow to cool below 75 °C
11. Extract sample, allow to cool to room temperature, and label it.

Appendix F: Bulk Specific Gravity (BSG) of Compacted Samples

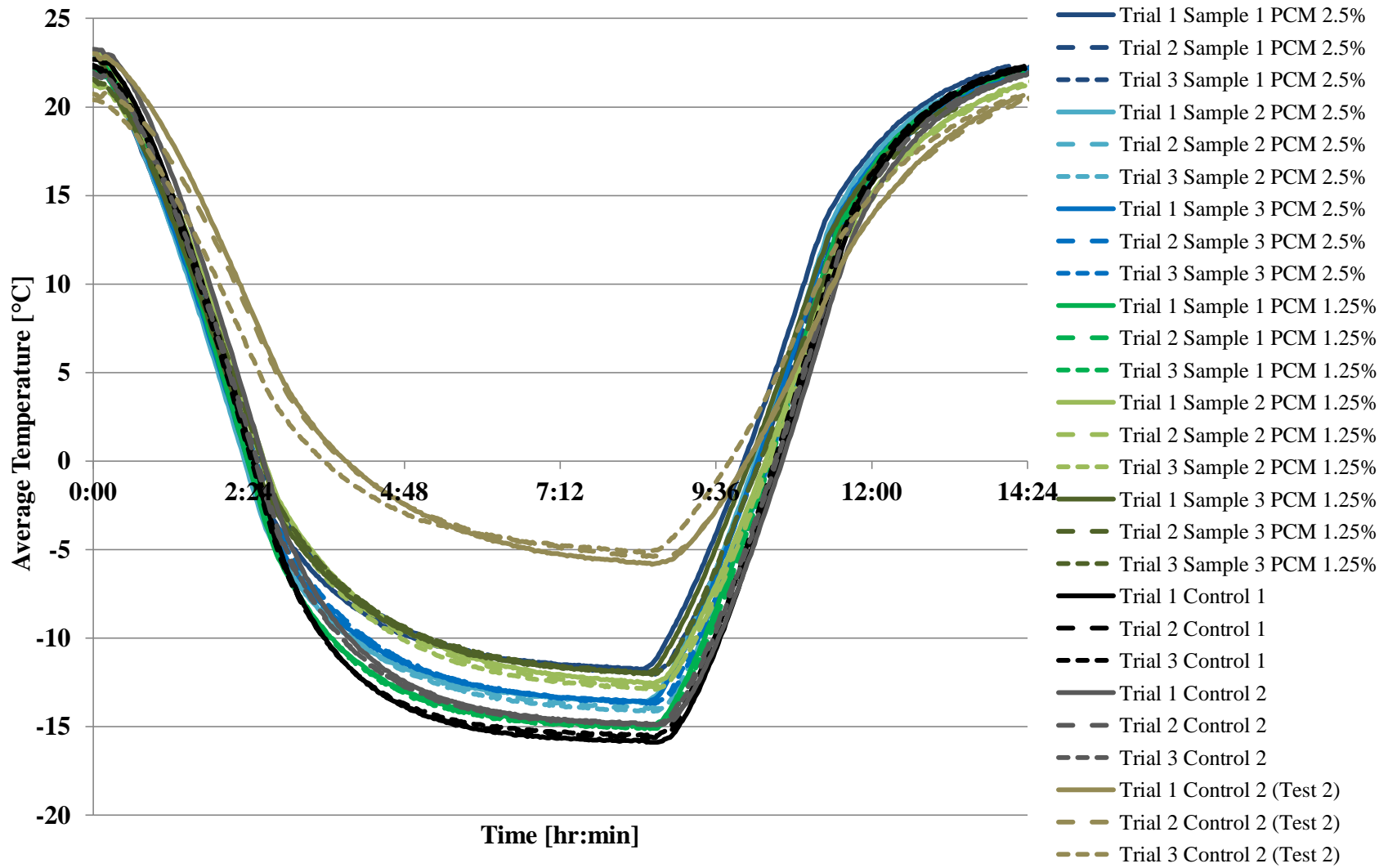
NOTE: The compacted sample must be dry and cooled to room temperature for accurate and repeatable results.

1. Turn CoreLok on and set to Program 1
2. Select a bag (note size), record mass of bag, and place it on the sliding plate with the opening facing the seal bar.
3. Remove any sharp edges from the sample in order to prevent punctures during the test.
4. Weigh the sample and record dry sample weight
5. Place the sample in the bag on top of the sliding plate (the sample should not touch the lid when closed).
6. Close lid and wait for the CoreLok to run
7. When finished, remove and inspect sample for proper sealing, the bag should be tight around the sample.
8. Place the sample on the weight basket gently (make sure it does not fall off) and wait for the scale to stabilize, record the submerged weight.
9. Remove the sample, inspect for water, and remove the sample from the bag (be careful not to get water on the sample). Determine the mass of the sample after submersion; if the weight of the sample has increased the test must be re-run.
10. Calculate the bulk specific gravity

Appendix G: Raw Data for Absorption of PCM-6 into LWA

Sieve-Trial	Mesh (g)	Mesh+LWA (g)	Mesh+LWA+PCM (g)	LWA (g)	PCM (g)	LWA/PCM Percentage (%)
#4-1	1.87	5.92	6.33	4.05	0.41	10.1
#4-2	1.60	5.30	5.69	3.70	0.39	10.5
#4-3	1.90	6.42	6.88	4.52	0.46	10.2
#4-1	1.88	6.98	7.47	5.1	0.49	9.6
#4-2	1.6	6.23	6.66	4.63	0.43	9.3
#4-3	1.9	6.13	6.58	4.23	0.45	10.6
#8-1	1.87	5.54	6.06	3.67	0.52	14.2
#8-2	1.90	5.35	5.79	3.45	0.44	12.8
#8-3	1.97	4.99	5.39	3.02	0.40	13.3
#8-1	1.87	5.59	6.08	3.72	0.49	13.2
#8-2	1.89	5.12	5.55	3.23	0.43	13.3
#8-3	1.96	5.82	6.31	3.86	0.49	12.7
#16-1	1.63	4.43	4.95	2.80	0.52	18.6
#16-2	1.70	4.79	5.36	3.09	0.57	18.5
#16-3	1.96	4.59	5.06	2.63	0.47	17.9
#16-1	1.63	4.08	4.51	2.45	0.43	17.6
#16-2	1.69	4.51	5.04	2.82	0.53	18.8
#16-3	1.95	4.39	4.81	2.44	0.42	17.2
Blend-1	1.88	7.47	8.16	5.59	0.69	12.3
Blend-2	1.96	7.34	7.97	5.38	0.63	11.7
Blend-3	1.91	6.35	6.88	4.44	0.53	11.9
Blend-1	1.87	7.47	8.12	5.60	0.65	11.6
Blend-2	1.95	7.05	7.67	5.10	0.62	12.2
Blend-3	1.89	7.22	7.85	5.33	0.63	11.8

Appendix H: Temperature Profiles for all Phase 2 GLC Trials



Appendix I: Calculations for Theoretical Maximum Density (TMD) Test

Sample ID	A Bag Weight (g)	B Weight of Rubber Sheets (g) (0 if not used)	Bag and sample weight (g)	C Weight of Sample in Air (g)	D Weight of Bags and Sample in Water (g)	E Total Volume (A+B+C)-D	F Bag and Rubber Sheet Volume A/Vc+B/Rc	G Sample Volume E-F	H Density C/G (g/cm ³)
Control 2-1	75.00	0	363.3	288.30	155	208.30	83.06	125.24	2.30
Control 2-2	75.60	0	343.2	267.60	147.50	195.70	83.72	111.98	2.39
Control 2-3	74.80	0	343.0	268.20	146.3	196.70	82.83	113.87	2.36
Control 2-1	74.8	0	363	288.20	154.3	208.70	82.83	125.87	2.29
Control 2-2	74.4	0	342.4	268.00	138.3	204.10	82.39	121.71	2.20
Control 2-3	75.1	0	345.1	270.00	154.5	190.60	83.17	107.43	2.51
								Avg TMD	2.34
								St Dev	0.11

Constants	g/cm ³
Rc	n/a
Vc	0.903

Appendix J: Volumetric Property Calculations

Sample ID	A Bag Weight (g)	B Dry Sample Weight before Sealing (g)	C Sealed Sample Weight in Water (g)	D Dry Sample Weight After Water Submersion (g)	E Ratio B/A	F Bag Apparent Gravity from Table	G Total Volume (A+D) - C	H Volume of Bag A/F	I Volume of Sample G-H	J Bulk Specific Gravity B/I
Control 2-4	85.5	278.3	106.2	278.1	3.3	0.8079	257.4	105.8	151.6	1.836
Control 2-5	91.0	266.1	113.6	266.1	2.9	0.8086	243.5	112.5	131.0	2.032
Control 2-6	91.9	271.6	116.1	271.6	3.0	0.8085	247.4	113.7	133.7	2.031
PCM 1.25-1	91.8	254.3	99.3	254.3	2.8	0.8090	246.8	113.5	133.3	1.907
PCM 1.25-2	91.4	252.7	99.4	252.7	2.8	0.8090	244.7	113.0	131.7	1.919
PCM 1.25-3	91.3	259.7	103.7	259.7	2.8	0.8088	247.3	112.9	134.4	1.932

Sample ID	Mass Agg (g)	Mass Binder (g)	P _b	P _s	G _{mb}	VTM (%)	VMA (%)	VFA (%)
Control 2-4	279.5	16.4	5.5	94.5	1.84	21.5	35.8	39.8
Control 2-5	278.7	15.6	5.3	94.7	2.03	13.2	28.7	54.2
Control 2-6	280.3	15.5	5.2	94.8	2.03	13.2	28.7	54.0
Averages					1.97	16.0	31.1	49.3
Standard Deviations					0.11	4.8	4.1	8.3

PCM 1.25-1	267.3	14.8	5.2	94.8	1.91	16.7	33.1	49.5
PCM 1.25-2	269.0	15.6	5.5	94.5	1.92	16.2	32.8	50.6
PCM 1.25-3	267.0	14.8	5.3	94.7	1.93	15.6	32.2	51.5
Averages					1.92	16.2	32.7	50.5
Standard Deviations					0.01	0.5	0.4	1.0